Journal of Engineering Physics and Thermophysics, Vol. 77, No. 3, 2004

THE CONSTANT OF THERMAL DESTRUCTION AND ITS ROLE IN THE PROCESSES OF HEATING AND ENTRAINMENT OF MASS OF A MATERIAL

G. A. Frolov

UDC 536.2.083

A model of heating and thermal destruction of a material is suggested on the basis of analysis and generalization of computational-experimental and literature data. The fundamental importance of the constant of thermal destruction in nonstationary processes of heating and entrainment of mass and its interrelation with the heat of material evaporation are shown. The mechanism of heat absorption in the surface layer of the destructing material, which determines the time of reaching the quasistationary mode of heating and entrainment of mass, is found. The limiting power capacity of internal and surface processes of heat absorption by a heat-protective material is considered.

Introduction. Recently, a large number of different heat-protective materials have been developed for thermally stressed elements of rocket-space equipment, including space apparatuses entering the atmospheres of planets at the second or higher space velocities. However, the possibilities of developing a heat-protective material capable of resisting high thermal loads with a minimum mass loss have fallen far short of being exhausted.

It is necessary to know the amount of thermal energy absorbed in destruction of material in both estimation of the efficiency of the heat-protective coating (the more the better) and calculation of the economy of the processes of, e.g., electric slag remelting, welding, and cutting of different materials.

In the present paper, based on the experimental results obtained on high-temperature benches and setups of the Institute of Problems of Material Science of the National Academy of Sciences of Ukraine [1–4] and the analysis of generalization of the literature data, we showed the fundamental importance of the constant of thermal destruction K_{T_d} in nonstationary processes of heating and entrainment of mass, which was first found in [5], and its interrelation with the heat of material evaporation. As the material–standard for computational-experimental studies we took doped quartz glass-ceramic (QGC), which is opaque under the conditions of convective heating and in which binder is absent. Moreover, Yu. V. Polezhaev has developed models of fusion with and without account for the viscosity for quartz-glass-based materials and performed a wealth of numerical calculations within a wide range of thermophysical properties of these materials and parameters of the oncoming gas flow [6].

For calculation of the heat flux spent for heating of the inner layers in a heat-protective material (HPM) without internal conversions use is usually made of the nonstationary heat-conduction equation in the form

$$\rho c \frac{\partial T}{\partial \tau} = \rho c V_\infty \frac{\partial T}{\partial y} + \frac{\partial}{\partial y}\left(\lambda \frac{\partial T}{\partial y}\right) \tag{1}$$

with boundary and initial conditions:

1) at $\tau = 0$, $T(y) = T_0 = \text{const}$, $V_\infty = 0$;

2) for $\tau > 0$ and $y = 0$

$$q_0 + q_{\text{rad}} = \varepsilon\sigma T_{\text{w}}^4 + \Gamma G_\Sigma \Delta Q_{\text{w}} + q_{\text{inj}} - \left(\lambda \frac{\partial T}{\partial y}\right)_{\text{w}}; \tag{2}$$

3) for $\tau > 0$ and $y \to \infty$ $T \to T_0$;

I. N. Frantsevich Institute of Problems of Material Science, National Academy of Sciences of Ukraine, 3 Krzhizhanovskii Str., Kiev, 03142, Ukraine; email: frolov@alfacom.net. Translated from Inzhenerno-Fizicheskii Zhurnal, Vol. 77, No. 3, pp. 19–46, May–June, 2004. Original article submitted November 28, 2002; revision submitted April 18, 2003.

1062-0125/04/7703-0489

4) for $T \to \infty$

$$-\left(\lambda \frac{\partial T}{\partial y}\right)_w = \rho \bar{V}_\infty c_p (T_w - T_0) = \rho \bar{V}_\infty H (T_w) . \quad (3)$$

The boundary condition in calculation of material heating by (1) is the equation of heat balance (2), which involves the following factors of absorption and scattering of convective q_0 and radiative q_{rad} heat fluxes that are supplied from outside to the material surface: removal of heat for heating of inner layers, radiation from the surface $\varepsilon\sigma T_w^4$, thermal effects of surface conversions ΔQ_w, and the effect of injection q_{inj}, which increases with an increase in the rate of destruction and enthalpy of the delayed flow and is assumed to be the most energy-consuming process [6]. Each of these factors, to greater or lesser extent, depends on both the material properties and the parameters of the oncoming gas flow and can change virtually from zero to its maximum value.

When the mass is carried away from the outer surface of the material the possibility of reaching the quasistationary mode of heating exists. The most important special features of it are the fact that the temperature profile in the body ceases to change with time and the heat flux spent for heating of the inner layers is no longer dependent on the coefficient of heat conduction near the surface and is stipulated by heat capacity of the heated layer (3). In this case, the rate of mass entrainment for $\gamma \bar{G}_w < 0.4$ can be calculated by an equation which follows from the equation of heat balance (2) on the surface of the destructing material:

$$G_\Sigma = \frac{q_0 + \varepsilon (q_{rad} - \sigma T_w^4)}{\Gamma [\Delta Q_w + \gamma (I_e - I_w)] + H (T_w)} . \quad (4)$$

In order to determine the rate by (4) we must know the total thermal effect of physicochemical processes on the surface ΔQ_w and the coefficient of gasification Γ. In determining ΔQ_w we have to consider numerous chemical reactions on the destructing surface of the material. Only in some cases do we succeed in obtaining analytical formulas for calculation of the composition of the gas and, correspondingly, completing the problem of determination of ΔQ_w [6]. No lesser difficulties emerge in calculation of the degree of realization of heat ΔQ_w which is determined by the coefficient of gasification Γ. Therefore, the denominator of Eq. (4) is given the name of effective enthalpy of the material, which is calculated on the basis of the experimental data.

If the parameters of the external effect and the effective enthalpy are known, the thickness of the entrained layer is usually determined by the formula

$$S (\tau) = \int_{\tau_1}^{\tau_2} \frac{q_0 - \varepsilon\sigma T_w^4}{\rho I_{eff}} , \quad (5)$$

which does not take into account the period of time τ_v necessary for establishing the quasistationary rate of entrainment by the value of which I_{eff} is calculated. Thus, an error is introduced the value of which can amount to tens of percent depending on the conditions of heating.

The results of experimental studies of heat-protective materials are usually generalized by the dimensionless rate of mass entrainment [6], the use of which allows one to eliminate the heat-transfer coefficient $(\alpha / c_p)_0$ from consideration:

$$\bar{G}_\Sigma = \frac{G_\Sigma}{(\alpha / c_p)_0} . \quad (6)$$

However, in order to determine the characteristics of a heat-protective material (effective enthalpy, thermophysical properties, rate of entrainment, etc.) experimentally and to study the dynamics of nonstationary processes we must find the length of the nonstationary period. It is usually supposed that the surface temperature, the rate of entrainment, and the length of the heated layer approach their stationary values asymptotically [6]; therefore, estimation

of the length of the nonstationary period requires assignment of the degree of approximation to the asymptote $\Delta\varepsilon$. For example, the accuracy of determination of the time of reaching the quasistationary rate of mass entrainment τ_v is specified by the quantity $\Delta\varepsilon > 0$ at which the relation $\left|[\overline{V}_\infty - V_\infty]/\overline{V}_\infty\right| < \Delta\varepsilon$ holds. In [6] it is stated that the dependence of τ_v on $\Delta\varepsilon$ is rather strong (an increase in the degree of approximation to the asymptote from 0.1 to 0.05 requires an almost twofold increase in the time of heating τ_v). A similar approach is used in determining the times of attainment of quasistationary values of the surface temperature τ_T and thickness of the heated layer τ_δ.

Self-Similar Mode of Heating in Entrainment of Mass from the Surface of a Heat-Protective Material. In the classical theory of heat conduction, wide use is made of the concept of a self-similar mode of heating when the Fourier number is the only variable that determines the process of heat propagation [7]. At T_w = const

$$\theta^* = \frac{T^* - T_0}{T_w - T_0} = \operatorname{erfc}\left(\frac{y}{2\sqrt{a\tau}}\right). \tag{7}$$

In this case, the depth of the heated layer δ obeys the relation $\delta = K\sqrt{a\tau}$, where K is the coefficient characterizing the velocity of movement of different isotherms, i.e., K depends on θ^*. It is assumed that for establishment of this mode it is requisite that the temperature of the outer heated surface should be constant and surface entrainment either should be absent or its rate should be in inverse proportion to the square root of the time of heating. However, measurements of the distance from the initial surface of the specimen to the isotherm of coking after testing of specimens at different times of heating [8] and processing of x-ray photographs obtained by the pulsed x-ray diffraction method in [9] showed that the path of this isotherm increases in direct proportion to the square root of the time of heating. This conclusion was confirmed by studies of specimens made of doped quartz glass-ceramic where movement of the isotherm T^* = 1800 K, which corresponded to the change in the color of the initial material [10, 11], was monitored and thermocouple measurements were conducted [12]. Thus, the change in the total thickness of the heated and entrained layers Δ^* can be calculated by the formula

$$\Delta^* = K\sqrt{a}\,(\sqrt{\tau} - \sqrt{\tau_\xi}), \tag{8}$$

and the velocity of movement of the isotherm T^*, which bounds the heated layer, by the expression

$$V_{\theta^*} = \frac{K\sqrt{a}}{2\sqrt{\tau}}. \tag{9}$$

Here $\sqrt{\tau_\xi}$ is the section that is cut off by the linear relation (8) on the abscissa axis.

Polezhaev and Frolov [5] found experimentally that for $\theta^* < 0.2$–0.3 satisfactory agreement between the calculation and experiment is given by (7) and for $\theta^* > 0.2$ it is better to use the equation

$$K = -\frac{1}{K_{T_d}}\theta^* + \frac{K_{T_d}^2}{1 - K_{T_d}}. \tag{10}$$

Only one value of K_{T_d} is possible in expression (10). At θ^* = 1 it passes to the third-power equation

$$2K_{T_d}^3 - K_{T_d}^2 + K_{T_d} - 1 = 0, \tag{11}$$

whose solution gives a numerical value of the constant of thermal destruction $K_{T_d} \approx 0.74$.

Thus, we have shown that the total thickness of the heated and entrainment layers $\Delta^* = S(\tau) + \delta_T(\tau) \approx K\sqrt{a\tau}$, where, in contrast to the classical self-similar solution, $K \neq 0$ even at θ^* = 1 although due to the fact that the isotherm moves relative to the initial size of the body.

To draw further conclusions it is worth noting that Eq. (11) gives several relations that differ by unity and that were used in obtaining the corresponding computation relations

$$\frac{K_{T_d}}{(K_{T_d}^2+1)(1-K_{T_d})}=\frac{1}{K_{T_d}^2}=1.831\,,\quad \frac{K_{T_d}^2+1}{K_{T_d}^2}=\frac{K_{T_d}}{1-K_{T_d}}=2.831\,,\quad \frac{K_{T_d}^2+1}{K_{T_d}^3}=\frac{1}{1-K_{T_d}}=3.831\,.$$

In [13], a model of thermal destruction of a material is suggested; this model allowed obtaining formulas for determination of the time of onset of surface destruction

$$\tau_d=\frac{K_{T_d}^6 a}{4\,(K_{T_d}^2+1)^2\,\bar{V}_\infty^2}\,, \tag{12}$$

the time of establishment of a stationary rate of mass entrainment

$$\tau_v=\frac{K_{T_d}^2 a}{4\bar{V}_\infty^2} \tag{13}$$

and linear entrainment at this instant of time

$$S(\tau_v)=\frac{K_{T_d}^2 a}{4(K_{T_d}^2+1)\,\bar{V}_\infty}\,. \tag{14}$$

However, it is difficult to use Eqs. (12)–(14) in calculations, since determination of the thermal diffusivity a at the temperature of surface destruction can be a major challenge.

The Parameter of Nonstationary Entrainment of Mass. In experimental studies, the velocity of HPM entrainment is often found by measuring linear entrainment as a function of the time of heating. In this case, processing of the results for $\tau>\tau_v$ by the least-squares method allows one to obtain the equation for linear entrainment in the form

$$S(\tau)=\bar{V}_\infty\tau-d_0\,. \tag{15}$$

In [14, 15], the dependence of the parameter d_0 on the class of material, type of heating, and thermophysical and physicochemical characteristics of a material was studied experimentally and numerically. For example, doped and pure quartz glass-ceramic, quartz glass, glass-reinforced plastic, asbestos textolite, and graphite were tested in radiative, convective, and combined radiative-convective types of heating within the range of heat fluxes from 6000 to 50,000 kW/m^2 and stagnation enthalpy from 4000 to 40,000 kJ/kg. In calculations, values of the density, viscosity, heat capacity, fraction of evaporation, pressure gradient, aerodynamic friction, emissivity, heat of evaporation, and thermal conductivity of material varied within a wide range. To determine the dependence of d_0 values on the characteristics of the material and parameters of heating we used the curves of linear entrainment calculated by Yu. V. Polezhaev by the model of quartz glass fusion with account for viscosity [6]. Graphical determination of d_0 by the computational curves of linear entrainment $S(\tau)$ does not require assignment of the degree of approach to the asymptote $\Delta\varepsilon$. These studies showed that d_0 weakly depends on the conditions of heating and all parameters of the material, except for the thermal conductivity of it.

Since Eq. (15) holds from the instant of time τ_v, substitution of (13) and (14) into it yields

$$\tau_v=\frac{K_{T_d}^2+1}{K_{T_d}^2}\,\frac{d_0}{\bar{V}_\infty}\,, \tag{16}$$

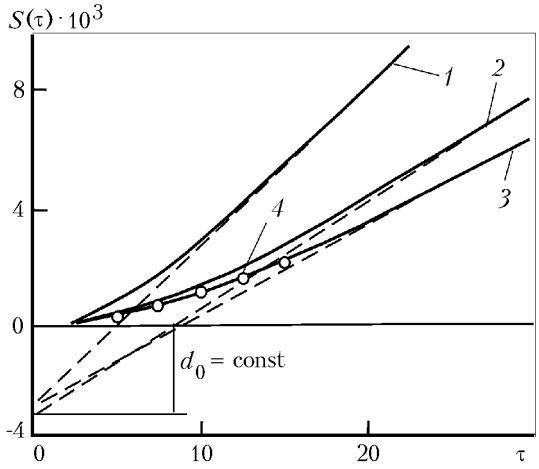

Fig. 1. Dependence of linear entrainment of quartz glass (λ = 10.4 W/(m·K)) on the time of heating (P_e = 0.13·10^5 Pa, I_e = 20,000 kJ/kg): 1–3) calculation by the model of quartz glass fusion [6] with different laws of variation of its viscosity (curves 1–3, Fig. 2 [15]) and by formula (19); 4) experiment [16]; dashed lines — stationary mode of mass entrainment. $S(\tau)$, m; τ, sec.

$$S(\tau_v) = \frac{d_0}{K_{T_d}^2}. \tag{17}$$

The parameter of nonstationary entrainment of mass d_0 turned out to be no less interesting than the constant of thermal destruction K_{T_d}, since it allowed one to do without determination of high-temperature thermal conductivity of the material in calculation of nonstationary destruction of the surface.

Nonstationary Destruction of an HPM Surface with a Variable Thermal Effect. Since the constant K_{T_d} affects the velocity of motion of surface isotherms, which in the nonstationary regime is related to V_∞ in terms of thermal conductivity (or the parameter d_0), we can expect the existence of an interrelation between them. Actually, processing of experimental data on linear entrainment for quartz-glass-based materials at the nonstationary stage [13, 16, 17] and results of the numerical calculations by the model of melting of quartz glass with account for viscosity [6] in the form

$$\frac{V_\infty}{\overline{V}_\infty} = f\left(\frac{\tau - \tau_{ent}}{\tau_v - \tau_{ent}}\right)$$

showed that, although in the experiments and calculations the fraction of material evaporation changed from 0.1 to 0.8, all the results obtained lie within a comparatively narrow range. In this case, the curve that approximates them gives the value

$$\int_0^1 (V_\infty/\overline{V}_\infty)\, dt \approx 0.74 = K_{T_d}, \quad t = \frac{\tau - \tau_{ent}}{\tau_v - \tau_{ent}}. \tag{18}$$

Moreover, it is shown in [13] that experimental data on the thickness of the entrained layer at the nonstationary stage are in satisfactory agreement with calculation by the expression

$$S(\tau) = \left\{\frac{\sqrt{\tau} - \sqrt{\tau_{ent}}}{\sqrt{\tau_v} - \sqrt{\tau_{ent}}}\right\}^2 S(\tau_v). \tag{19}$$

Differentiation of Eq. (19) and substitution of (12)–(14) in it also give a value of $K_{T_d} \approx 0.74$.

Figure 1 presents the results of numerical calculation by the model of quartz glass fusion [6], which almost completely coincide with calculation by formula (19) if Eqs. (16) and (17) are used for determination of $S(\tau_v)$ and τ_v. Despite the complex character of variation of the effective thermal conductivity of quartz glass at high temperatures, experimental dependences of linear entrainment for this material are also in good agreement with calculation by the suggested equations and the corresponding parameter d_0, since this parameter integrates all nonstationary processes occurring in the surface layer of the destructing material.

In the general case, the time of onset of mass entrainment does not coincide with the time of onset of destruction, for example, fusion of the quartz-glass ceramic surface ($\tau_{ent} \neq \tau_d$) [10]. However, in practical calculations this discrepancy can be neglected. Therefore, for determination of $\tau_{ent} = \tau_d$ the results obtained in [6] are suitable; it follows from these results that in practice the range of variation of thermal efficiency of the material ($m = c(T_d - T_0)/\Delta Q$) can be limited within $0.5 < m < 3$. Within this range, the ratio τ_v/τ_d changes from about 6 to 10 and its mean value is 8.

Equations (16)–(19) and the parameter d_0 are assigned at constant thermal load. However, this does not eliminate their use in the case of a variable heat flux (for example, Fig. 2), if, as in the case of formula (5), the real curve $q_0(\tau)$ is substituted by an approximating stepwise dependence [18]. Then, for each kth step of heating, using the effective enthalpy and a steady-state value of the surface temperature and formula (19) we can calculate the rate of entrainment and determine the values of τ_{entk} and τ_{vk} necessary for calculation. The equation for calculation of linear entrainment on the kth section of heating, when entrainment in time τ_k (at the end of the kth step of heating) is $S(\tau_k) < S(\tau_v) = d_0/K_{T_d}^2$, has the form

$$S_k(\tau) = \left[\frac{\sqrt{\tau - \Delta\tau_k} - \sqrt{\tau_{entk}}}{\sqrt{\tau_{vk}} - \sqrt{\tau_{entk}}}\right]^2_{S(\tau)<S(\tau_v)} S(\tau_v), \quad \tau_{k-1} < \tau \le \tau_k . \tag{20}$$

Here $\Delta\tau_k = \tau_{k-1} - \left[\sqrt{\frac{S(\tau_{k-1})}{S(\tau_v)}}\,(\sqrt{\tau_{vk}} - \sqrt{\tau_{entk}}) + \sqrt{\tau_{entk}}\right]^2$ is the correction to the current time of heating τ on the kth section, which takes into account the layer entrained in the period of time $\tau_{k-1} - \tau_{ent1}$. For the first section of heating, $\Delta\tau_1 = 0$. When $S(\tau) \ge S(\tau_v)$, calculation is performed by the known formula

$$S(\tau) = \left|\sum_{i=1}^{n} \bar{V}_{\infty i}\Delta\tau_i\right|_{S(\tau)\ge S(\tau_v)} .$$

In Fig. 3, linear entrainment of quartz-glass ceramic calculated by (20) is compared to numerical calculation by Eq. (1), which at constant thermophysical properties has the form

$$\rho c\frac{\partial T}{\partial \tau} = \lambda\frac{\partial^2 T}{\partial y^2} + \rho c V_\infty\frac{\partial T}{\partial y} . \tag{21}$$

Here the rate of entrainment is determined from the equation of heat balance on the destructing surface of the material and is equal to

$$V_\infty = \frac{q_0 - \varepsilon\sigma T_w^4 - \lambda\left(\frac{\partial T}{\partial y}\right)_{y=0}}{\rho\Gamma\,[\Delta Q_w + \gamma(I_e - I_w)]} .$$

Numerical calculations are made at the following initial and boundary conditions:

1) at $\tau = 0$ $T(y) = T_0 = \text{const}$, $V_\infty = 0$;

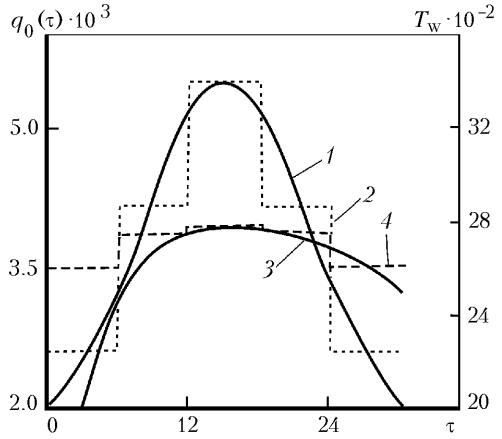

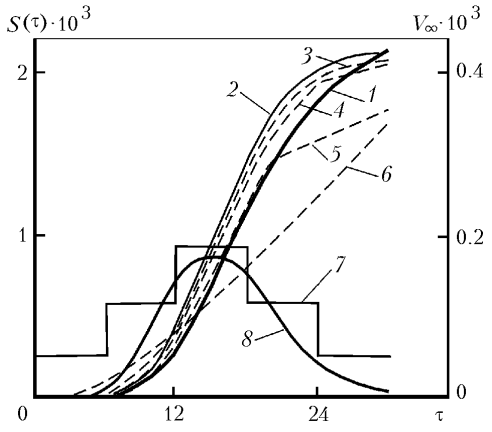

Fig. 2. Dependence of heat flux and surface temperature on the time of heating: 1) heat flux $q_0(\tau)$; 2) stepwise approximation of $q_0(\tau)$; 3) calculation of T_w with continuous variation of $q_0(\tau)$; 4) stationary values of T_w for each step of $q_0(\tau)$ variation. $q_0(\tau)$, kW/m^2; T_w, K; τ, sec.

Fig. 3. Dependence of linear entrainment $S(\tau)$ (curves 1–6) and velocity V_∞ (curves 7, 8) on the time of heating: 1) calculation by (20) using the parameter d_0 in five-step division into time intervals; 2–6, 8) calculation by (21); 2) continuous variation of $q_0(\tau)$; 3–6) nine-, five-, three-, and one-step approximation of $q_0(\tau)$; 7) stationary rate of entrainment, calculation by (4). $S(\tau)$, m; V_∞, m/sec; τ, sec.

2) at $\tau > 0$ and $y = 0$

$$\lambda\left(\frac{\partial T}{\partial y}\right)_w = G_w\Delta Q_w + \varepsilon\sigma T_w^4 = (\alpha/c_p)_w\,(I_e - I_w)\,,\quad G_w\,(\alpha/c_p)_w\,f\,(T_w, P_e)\,;$$

3) as $\tau > 0$ and $y \to \infty$, $T \to T_0$.

In the calculations it was taken that over a period of 30 sec the quartz-glass ceramic coating (λ = 2.1 W/(m·K), c_p = 1.26 kJ/(kg·K), ρ = 2000 kg/m^3, ΔQ_w = 11,000 kJ/kg, coefficient of gasification Γ = 0.6) is affected by the heat flux, which changes according to the law given in Fig. 2 at a constant value of the stagnation enthalpy of 10,000 kJ/kg. The parameter of nonstationary entrainment d_0 at λ = 2.1 W/(m·K), according to [15], is taken to be $1\cdot 10^{-3}$ m. The dependence of the evaporation rate G_w on the surface temperature and stagnation pressure is borrowed from [6].

If we disregard the nonstationary character of entrainment and determine it by the value $\overline{V}_\infty \sim 0.1\cdot 10^{-3}$ m/sec, which is the mean over the entire period of heating, it will exceed the actual value by 50%.

Calculation by (21) with account for stepwise and constant variations of $q_0(\tau)$ (Fig. 3, curves 2–6) showed that rather rough division into time intervals is possible in practice. Even with division of the dependence $q_0(\tau)$ into five constant intervals, the maximum difference of linear entrainment from calculation with constant variation of $q_0(\tau)$ does not exceed 10%.

Estimation of the Amount of Heat in the Surface Layer of the Material. During the time interval from τ_d to τ_T, due to accumulation of heat in the surface layer of the material the surface temperature increases from T_d to a stationary value $\overline{T}_w$. Since expression (8) holds only at T_w = const, we can assume that the coefficient K for θ^* = 1 is equal to K_{T_d} from the time instant τ_T. In [19], experimental values of the surface temperature within the range from T_d to $\overline{T}_w$ were given in the form

$$\frac{T_w - T_d}{\overline{T}_w - T_d} = \theta_{T_w} = f\,(t)\,,\quad t = \frac{\sqrt{\tau} - \sqrt{\tau_d}}{\sqrt{\tau_T} - \sqrt{\tau_d}}\,.$$

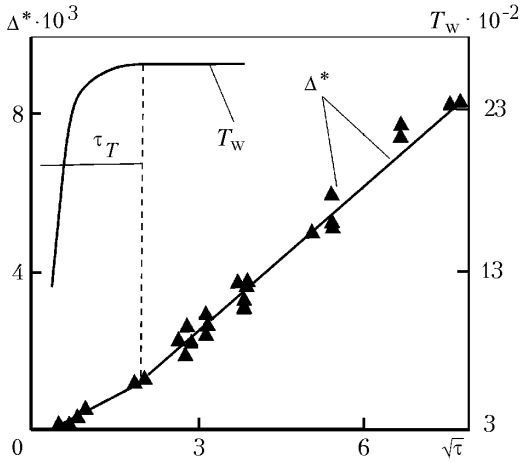

Fig. 4. Variation of the angle of inclination of the dependence $\Delta^* = f(\sqrt{\tau})$ for the isotherm $T^* = 1800$ K of doped quartz-glass ceramic at the instant of completion of heat accumulation in the surface layer (attainment of the stationary value of the surface temperature $\overline{T}_w$): dots — experimental data on heating of doped quartz-glass ceramic up to $T^* = 1800$ K. Δ^*, m; T_w, K; $\sqrt{\tau}$, $\text{sec}^{0.5}$.

These results are described by the polynomial to the fifth power

$$\theta_{T_w} = 1.480t^5 - 5.061t^4 + 7.377t^3 - 6.379t^2 + 3.581t + 9.690\cdot 10^{-3},$$

integration of which yields

$$\int_0^1 \theta_{T_w} dt = 0.742 \approx K_{T_d}.$$

Hence, we can see that the law of surface-temperature variation within the time range from τ_d to τ_T is also determined by the constant K_{T_d}. The results obtained allow us to draw the conclusion that a rather strict boundary between nonstationary and stationary modes exists in the process of thermal destruction of a material as well as in erosion entrainment of mass [20]. It follows from [21] that in erosion destruction, the "threshold" value of the mass of carried-away particles m^*_{er} upon attainment of which a stationary value of the rate of entrainment $\overline{V}_\infty$ is set is related to the rate of collision $\overline{V}_{er}$ by the equation

$$\frac{m^*_{er}\overline{V}^2_{er}}{2} = A.$$

The range of variation of the parameter A is comparatively narrow and for nonmetallic materials it can be taken equal to 10^6 J/m^2. To the instant when the amount of energy supplied to the material surface reaches A the process of establishment of the stationary mode of erosion entrainment of mass is completed. In thermal destruction, a great part of the heat (energy) entering the body is removed due to heat conduction into the depth of the material. Therefore, there is no sense in speaking of the amount of heat, which is constant for all the cases. However, taking into account the analogy between thermal and erosion destruction of materials [20], we can assume that the process mentioned manifests itself in thermal entrainment of mass as well. Estimation of the amount of heat absorbed in the surface layer at the instant of establishment of the surface temperature shows that for graphite this quantity is of about 6000 kJ/m^2 (thermal diffusivity $a = 15\cdot 10^{-6}$ m^2/sec) and for doped quartz-glass ceramic ($a = 0.65\cdot 10^{-6}$ m^2/sec) it is of about 1000 kJ/m^2.

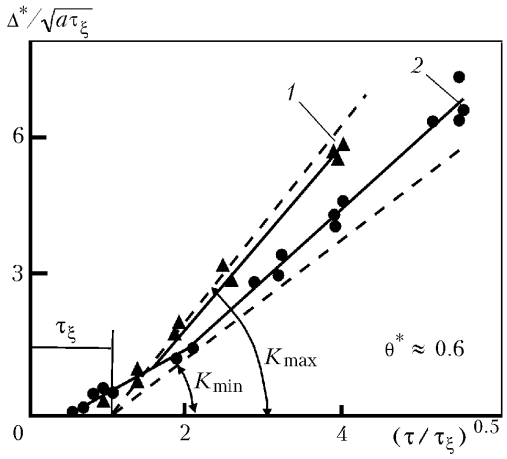

Fig. 5. Influence of the rate of entrainment on the coefficient K (dots — experimental data on heating of doped quartz-glass ceramic up to $T^* = 1800$ K): 1) dimensionless rate of entrainment $V_\infty = 0.26$; 2) 0.14; the lower dashed line — calculation of K by Eq. (10); the upper dashed line — calculation by (29).

Probably, as the thermal diffusivity of the material decreases, the amount of heat absorbed in the destructing layer to the moment when the surface temperature is established tends to the value of the parameter A obtained for nonmetallic materials in the case of erosion destruction.

Thus, the constant of thermal destruction of the material K_{T_d} affects the laws of variation of the surface temperature, the rate of mass entrainment, and movement of isotherms of the temperature field and determines the amount of heat absorbed in the surface layer of the destructing material. The moment of attainment of $\bar{T}_w$ coincides with completion of the process of heat accumulation and reflects on the laws governing the movement of high-temperature isotherms — linear dependence (8) changes the angle of inclination rather sharply (Fig. 4).

In further studies of temperature fields in quartz-glass ceramic, including movement of the isotherm corresponding to a change in color in doped quartz-glass ceramic, we found a great dependence of the coefficient K in (8) on the rate of mass entrainment (Fig. 5). As is seen from the figure, heat flux supplied to the surface affects the coefficient K (i.e., the velocity of movement of isotherms) only upon completion of the mentioned process of heat absorption in the surface layer of the destructing material.

We studied the reason for the origination of the total "focus" of the linear dependence (8), which was equal to the square root of one second virtually for all experiments and different heat-protective materials, for example, in [8, 12]. Although numerical calculations of heating by (1) with the boundary conditions on the surface (rate of entrainment and surface temperature) determined by the constant K_{T_d} are in agreement with the experiment only up to $\theta^* \le 0.3$, they confirm the experimental data given in Figs. 4 and 5 and indicate that displacement of the curves $\Delta^* = f(\sqrt{\tau})$ along the abscissa axis by a value $\sim\sqrt{1}$ sec$^{0.5}$ is a consequence of variation of the rate of entrainment and surface temperature by the laws obtained on the basis of the constant K_{T_d} in [13, 19].

Ultimate Energy Capacity of Internal Processes of Heat Absorption. In practice, by the depth of the heated layer (the necessary thickness of the heat-protective coating) we mean the distance from the heated surface to some determined plane $T^* = \text{const}$. Usually, of the entire set the isotherm with dimensionless temperature $\theta^* = 0.05$ [22] or $\theta^* = 0.1$ [6] is distinguished. However, the heated layer can be bounded by an isotherm with any T^* that is lower than the temperature of the heated surface. At high rates of heating, the surface temperature increases quickly to a value T_d and in some time reaches a stationary value $\bar{T}_w$. At this instant of time, the temperature field is similar to a compressed spring where the coils represent the isotherms of the temperature field. If we release one end of the spring, the path passed by each coil of it will be the larger the more the distance from the motionless end of the spring. As the temperature of the considered isotherm decreases, its velocity increases and to the moment of establishment of the quasistationary mode of heating τ_δ the path passed by this isotherm will be the higher the smaller its temperature. At this instant of time, the heated layer reaches a maximum value and the amount of heat accumulated in it reaches a limiting value. As the thermal effect continues, all isotherms whose temperature is higher than a value

TABLE 1. Comparison of Experimental and Calculated Values of the Depths of Heating up to the Isotherm T^* = 1800 K in the Specimens of Doped Quartz-Glass Ceramic [1) experiment; 2) calculation by (27)]

$a\cdot10^6$, m^2/sec	q_{cal}, kW/m^2	I_e, kJ/kg	T_w, K	$\bar{V}_\infty\cdot10^3$, m/sec	$\delta_T\cdot10^3$, m	
					1	2
0.65	7650	8600	2620	0.10	2.65	2.83
0.65	10,500	10,600	2710	0.16	2.0	1.93
0.65	10,500	12,300	2800	0.16	2.2	2.08
0.65	11,500	12,300	2800	0.18	1.75	1.84
0.65	14,000	12,300	2820	0.21	1.6	1.61
0.45	7000	3500	2400	0.09	1.5	1.68
0.45	14,000	4700	2530	0.14	1.3	1.27

Note: Experimental values of δ_T are obtained by processing of at least 10 experiments in each mode of heating.

T^* which bounds the heated layer will move at a velocity equal to the stationary rate of destruction of the material surface.

Polezhaev and Yurevich [6] derived a formula for calculation of the stationary value of the depth of the heated layer:

$$\delta_T = \frac{a}{\bar{V}_\infty} \ln \frac{T_w - T_0}{T^* - T_0}. \tag{22}$$

On the other hand, Eqs. (8) and (15) allow one to obtain one more expression for calculation of the stationary value of the depth of heating. With this in mind, we present (8), (9), (15), and (22) in dimensionless form:

$$\Delta^*(t) = K\sqrt{t} - 1, \tag{23}$$

$$S(t) = \bar{\bar{V}}_\infty t - \bar{d}_0, \tag{24}$$

$$t_\delta = \frac{K^2}{4\bar{\bar{V}}_\infty^2}, \tag{25}$$

$$\bar{\delta}_T = -\frac{\ln\theta^*}{\bar{\bar{V}}_\infty}. \tag{26}$$

Here $S(t) = S(\tau)/\sqrt{a\tau_\xi}$; $\Delta^*(t) = \Delta^*/\sqrt{a\tau_\xi}$; $\bar{d}_0 = d_0/\sqrt{a\tau_\xi}$; $t = \tau/\tau_\xi$; $\bar{\bar{V}}_\infty = \bar{V}_\infty\sqrt{\tau_\xi/a}$.

As a result, we come to the expression

$$\bar{\delta}_T = \Delta^*(t_\delta) - S(t_\delta) = \frac{K^2}{4\bar{\bar{V}}_\infty} - K + \bar{d}_0. \tag{27}$$

Equating (26) and (27), we find an equation for determining the temperature coefficient:

$$K = 2\left\{\bar{\bar{V}}_\infty + \sqrt{\bar{\bar{V}}_\infty(\bar{\bar{V}}_\infty - \bar{d}_0) - \ln\theta^*}\right\}, \tag{28}$$

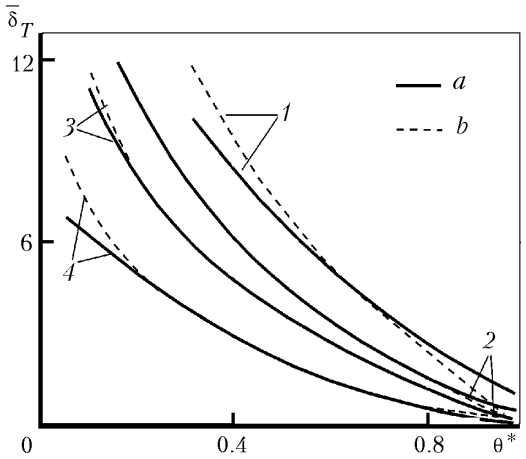

Fig. 6. Dependence of the heated layer on θ^* at different rates of entrainment: a) calculation by formula (27); b) (26); 1–4) dimensionless rate of entrainment $\bar{\bar{V}}_\infty$ = 0.1, 0.15, 0.2, and 0.32.

which is confirmed by experimental data within the range $0.1 \le \bar{\bar{V}}_\infty \le 0.3$ with variation of θ^* from 0.2 to 0.8 (e.g., Fig. 5).

The approaching of $\bar{\bar{V}}_\infty$ to a limiting value of ~0.3 leads to a strong decrease in the time of existence of linear dependences $\Delta^* = f(\sqrt{\tau})$. In this case, the rate of entrainment at which the regularity $\Delta^* = f(\sqrt{\tau})$ still holds will be the higher the larger the thermal diffusivity of the material. For example, for graphite ($a \approx 15 \cdot 10^{-6}$ m^2/sec) it can reach a value of $1 \cdot 10^{-3}$ m/sec. At $\bar{\bar{V}}_\infty \approx 0.3$, the nonstationary period for $\theta^* > 0.2$ can be neglected, and the coefficient K reaches maximum values:

$$K = -\left(\frac{1 - K_{T_d} + K_{T_d}^2}{1 - K_{T_d}}\right)\theta^* + \frac{1}{1 - K_{T_d}}. \tag{29}$$

It is of interest to note that if formula (10) at $\theta^* = 1$ changes over to a third-power equation solving which we find $K_{T_d} \approx 0.74$, then in Eq. (29) at $\theta^* = 1$ we obtain $K = K_{T_d}$, i.e., it degenerates.

Table 1 gives, in dimensional form, experimental and calculated values of the depth of the heated layer obtained by (27) using (28), and Fig. 6 presents a comparison of calculated dimensionless values of $\bar{\delta}_T$ found by (26) and (27).

To answer the question under which conditions is the limiting heat capacity of the internal processes of heat absorption reached, we use Eqs. (23)–(25). Substituting (25) into (23) and (24), we find that the relation

$$\frac{\Delta^*(t_\delta)}{S(t_\delta)} \approx 2 \tag{30}$$

holds with an accuracy to constants at the instant of time t_δ.

To eliminate the uncertainty in the choice of time t_δ, comparison of the thickness of the heated layer with a stationary value of $\bar{\delta}_T$ was made at the instant of time t_x when the heated-layer thickness was equal to linear entrainment. For this purpose, the time instant at which $S(t_x) = \delta(t_x)$ was determined by expressions (23) and (24).

Substituting the value of t_x into the equation of linear entrainment, as a result we come to a relation which makes it possible to find the applicability limits of regularity (30):

$$S(t_x) = \delta(t_x) = \frac{K}{2}\left(\frac{K}{4\bar{\bar{V}}_\infty} + \sqrt{\frac{1}{\bar{\bar{V}}_\infty}\left(\frac{K^2}{16\bar{\bar{V}}_\infty^2} - \frac{K}{\bar{\bar{V}}_\infty} + \bar{d}_0\right)} - 1\right). \tag{31}$$

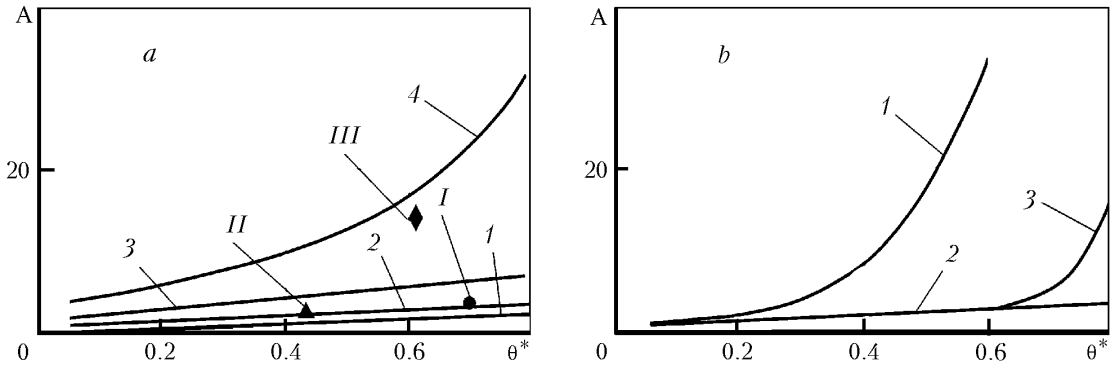

Fig. 7. Comparison of the thickness of the heated layer $\delta(t_x)$ at the instant of its equality to linear entrainment $S(t_x)$ with a stationary depth of heating $\bar{\delta}_T$: a) at different values of the rate $\bar{\bar{V}}_\infty$ and $\bar{d}_0 = 0.32$ [1–4) calculation, $\bar{\bar{V}}_\infty = 0.1$, 0.15, 0.2, and 0.3; I–III) experiment, $\bar{\bar{V}}_\infty = 0.124$, 0.14, and 0.26]; b) at different values of the parameter $\bar{d}_0$ and $\bar{\bar{V}}_\infty = 0.15$ [1) aluminum oxide, $\bar{d}_0 = 2.9$; 2) doped glass ceramic, $\bar{d}_0 = 0.32$; 3) graphite, $\bar{d}_0 = 1.16$]. $A = \left|[\delta_T - \delta(t_x)]/\delta_T\right|_{S(t_x)=\delta(t_x)}$, %.

Figure 7 gives calculations for the ratio $[\bar{\delta}_T - \delta(t_x)]/\bar{\delta}_T$ as a function of θ^*, the rate of entrainment $\bar{\bar{V}}_\infty$, and the parameter $\bar{d}_0$. It is seen that for rates $\bar{\bar{V}}_\infty < 0.2$ and $\bar{d}_0 < 0.1$ deviation of the heated-layer thickness at the instant of time t_x, when $S(t_x) = \delta(t_x)$, from the stationary value $\bar{\delta}_T$ does not exceed 8% for any value of θ^*. Only for rates $\bar{\bar{V}}_\infty > 0.3$ (for quartz-glass ceramic $\bar{G}_\Sigma > 0.5$) and $\bar{d}_0 > 1.0$ is this regularity violated. The results of the calculations are in good agreement with experimental data (dots in Fig. 7a).

The results obtained do not contradict the numerical calculations. For example, the model of heating and entrainment of mass from the surface of the crystal body [6] adequately confirms the linearity of the experimentally found regularity for the isotherms $\theta^* = 0.05$ and 0.1. Numerical calculations by this model show that, although mass entrainment and the heated-layer thickness change according to absolutely different laws, their total value during some period of time τ_δ, at which the equality of thicknesses of the heated and entrained layers is established, can be described (with good accuracy, ~5%) by the linear dependence

$$\Delta^*(t) = K\sqrt{t},$$

where $t = (\tau/\tau_d) - 1$ and the coefficient K is a function of dimensionless temperature θ^* and the thermal efficiency of the material $m = c(T_d - T_0)/\Delta Q$. Calculations also indicate that for the isotherms $\theta^* = 0.05$ and 0.1 at the instant when the thicknesses of the heated and entrained layers are equal the depth of the heated layer differs from its stationary value by no more than 10%.

However, the calculations allow such a conclusion only for isotherms with dimensionless temperatures $\theta^* \le 0.1$. At the same time, Fig. 8 presents experimental data that indicate the equality of thicknesses at the instant of time τ_δ even for the isotherm $\theta^* = 0.6$; in [20] it is shown that this regularity also holds in purely erosion destruction of material under the action of the flow of solid particles.

The regularity found is illustrated by the schematic presented in Fig. 9. It is seen that if a decrease in the velocity of shift from the minimum value to the stationary rate of mass entrainment is typical of the isotherms, the velocity of surface movement increases from 0 to $\bar{V}_\infty$. At the moment when the velocity of any isotherm decreases to the rate of surface destruction, the entrained layer thickness is equal to the depth of occurrence of this isotherm. The same conclusion follows from the example of a spring. If we imagine that the spring has the possibility of expanding to both sides (a part of the spring goes to the range of temperatures exceeding, for example, the temperature of melting or simply burns out), then at the moment of its full expansion the number of disappearing coils will be equal to one-half of the spring.

Hence it must follow that at the conditions of thermal effect under consideration the rate of mass entrainment does not depend on the thermal efficiency of the material (fraction of evaporation). The rate of material entrainment is

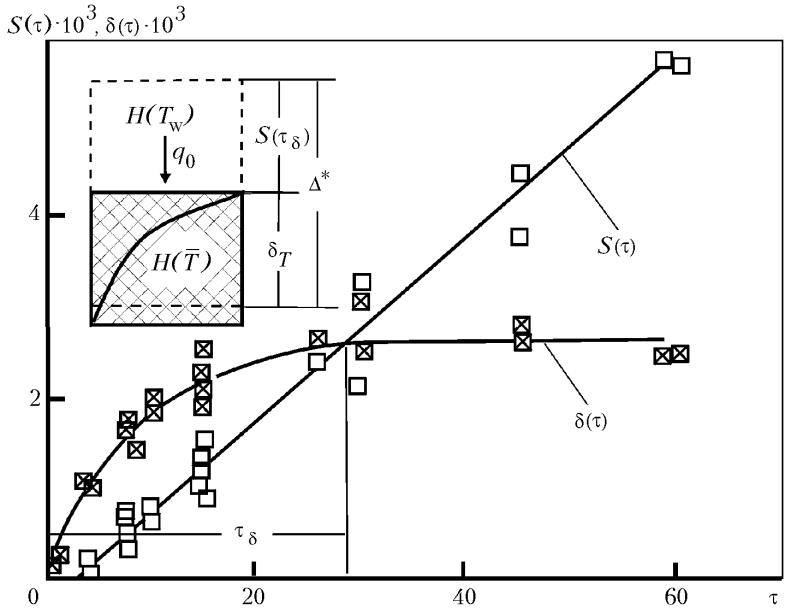

Fig. 8. Dependence of linear entrainment and the depth of heating on the time of heating for doped quartz-glass ceramic (q_{cal} = 7650 kW/m^2, I_e = 8600 kJ/kg, V_∞ = 0.1·10^{-3} m/sec); dots — experiment. $S(\tau)$, m; δ_T, m; τ, sec.

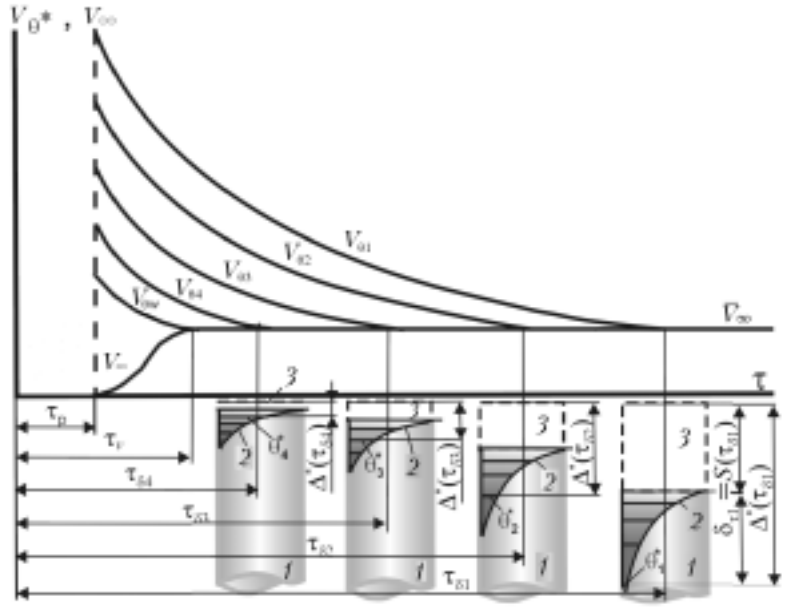

Fig. 9. The model of heating and entrainment of heat-protective material: 1) specimen; 2) temperature profile; 3) entrained layer; θ_1^*–θ_4^* — isotherms bounding the heated layer whose thickness is equal to the entrained layer. $\theta_1^* < \theta_2^* < \theta_3^* < \theta_4^* < \theta_w^* = 1$; $\delta_{\tau 1}$ — depth of the heated layer at time τ_1.

affected only by the value of the heat flux that determines the rate of surface heating before the onset of its destruction rather than by the total heat flux, which is established in the stationary mode of surface destruction. Actually, the experimental data given in [8] (Fig. 10) confirm this assumption.

Despite the fact that under different conditions of heating the rate of entrainment of asbestos textolite at the same thermal effect differed by about 3 times, the total thickness of the coked and entrained layers before establishment of the stationary mode of coking remained constant and increased in proportion to $\sqrt{\tau}$. The same conclusion

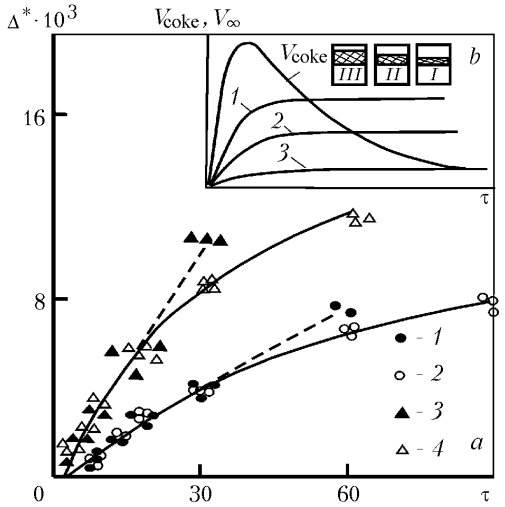

Fig. 10. Dependence of the total thickness of the coked and entrained layers on the time of heating (a) and the schematic of variation of the velocities of movement of the surface and front of coking in the samples of the material (b): a) [1, 3) convective heating in the air flow; 2, 4) radiative heating; 1, 2) heat flux 1600 kW/m^2; 3, 4) 10,000 kW/m^2; dashed lines — stationary mode of coking]; b) [1–3) velocity of movement of the material surface in heating in flows of air and nitrogen and in radiative heating; I–III) coked (cross-hatched) and entrained (clear) layers in the specimens of asbestos textolite after testing in flows of air and nitrogen and in radiative heating]. $\bar{T}_{wI} = \bar{T}_{wII} = \bar{T}_{wIII}$. Δ^*, m; τ, sec.

TABLE 2. Rate of Destruction of Doped Quartz-Glass Ceramic [1) experiment; 2) calculation by (4)]

q_{cal}, kW/m^2	I_e, kJ/kg	$P_e \cdot 10^{-5}$, Pa	T_w, K	q'_{mean}, kW/m^2	q'_0, kW/m^2	Γ	G_Σ, kg/(m^2·sec)	
							1	2
11,500	12,300	1.0	2800	9250	5550	0.82	0.36	0.34
14,700	4700	3.5	2610	8540	1530	0.1	0.36	0.38

follows from the experimental data given in Table 2. At almost the same integral-mean heat fluxes under the conditions of convective heating in the jet of combustion products from the gas generator and the air-plasma jet the same rates of destruction were obtained for specimens of doped quartz-glass ceramic, although heat fluxes in the stationary mode differed fivefold and the coefficient of gasification — eightfold. The latter was determined by the technique presented in [23, 24].

We consider heat balance at the moment of establishment of the quasistationary mode of heating τ_δ. If we neglect variation of heat flux in time τ_T, the heat balance can be written in the following form:

$$(q_0 - \varepsilon\sigma T_w^4)\,\tau_\delta = \rho\left\{\delta_T H(\bar{T}) + S(\tau_\delta)\,H(T_w) + \Gamma S(\tau_\delta)\,[\Delta Q_w + \gamma(I_e - I_w)]\right\}, \tag{32}$$

where

$$q_0 = q_{cal}\,\frac{I_e - I_w}{I_e - I_0}. \tag{33}$$

It is seen from Eq. (32) that a contradiction appears. On the one hand, the total thickness Δ^* involves linear entrainment of material and must depend on all terms of (32), including the coefficient of gasification; on the other hand, the relation $\Delta^*(t_\delta)/S(t_\delta) \approx 2$ is not connected with the thermal efficiency of the material.

In this case, it follows from (32) that relation (30) can hold either in complete absence of evaporation of the entrained material, i.e., at $\Gamma = 0$, or under the condition of, at least, a weak dependence of the rate of material entrainment on the fraction of evaporation. Fulfillment of the latter condition means that to one and the same rate of mass entrainment there must correspond virtually any value of the coefficient of gasification that satisfies the equation of heat balance (32). Numerical calculations [6] and experiments [23] show that the main changes in the coefficient of gasification and surface temperature occur within a comparatively small range of stagnation enthalpy. For example, for quartz glass this range is 4000–20,000 kJ/kg. In this range of enthalpy of the delayed flow, the coefficient of gasification changes from 0.1 to 0.9 and the surface temperature changes by about 300–400 K. This change of T_w slightly affects the heat capacity of the material but covers almost the entire range of rates of destruction of quartz-glass-based materials.

The heat flux supplied to the surface during the period of surface-temperature rise decreases from its calorimetric value q_{cal} to a value of q_0' ($q_0' = q_0 - \varepsilon\sigma T_w^4$) and then does not change any more. This change occurs mainly before the onset of destruction of the surface when its temperature increases from T_0 to $\overline{T}_w$. Therefore, we can assume that it is precisely the integral-mean value of heat flux during the period from 0 to τ_T that determines the rate of material surface heating.

The dependences of the surface temperature on the time of heating show that with an accuracy to 2% the integral-mean heat flux can be determined by the formula

$$q'_{mean} \approx \frac{q_{cal}}{2}\left(1 + \frac{I_e - I_w}{I_e - I_0}\right) - \frac{1}{4}\varepsilon\sigma T_w^4 . \tag{34}$$

If we neglect radiation and divide expression (34) by the heat-transfer coefficient, we can write

$$\overline{q}'_{mean} \approx 0.5\,(2I_e - I_w - I_0) \approx I_e - I_w , \tag{35}$$

i.e., in fact we come to a consideration of the values of the enthalpy difference in the boundary layer of the model ($I_e - I_w$), which differs from $\overline{q}'_{mean}$ in tests in plasma jets by no more than 5%.

Thus, the results obtained indicate that within the range of the enthalpy of the delayed flow, which corresponds to main variations of T_w and Γ ($I_e \le 15{,}000$ kJ/kg), the integral-mean heat flux in time from 0 to τ_T decisively affects the rate of surface destruction and the temperature field inside the material. The share of other factors of heat absorption in the total balance is specified by a value of the heat flux in the quasistationary mode of heating q_0' and increases with the stagnation enthalpy to 30%; in the range under consideration, the stagnation enthalpy weakly influences the rate of mass entrainment.

This conclusion is also confirmed by the fact that the stagnation enthalpy affects both the coefficient of gasification and q_0. Since in formula (33) $(I_e - I_w)/(I_e - I_0) < 1$, it is seen from (33) and (34) that the higher the stagnation enthalpy the smaller the difference between q'_{mean} and q_0', i.e., at least for quartz-glass ceramic the ratio q_0'/q'_{mean} is approximately equal to Γ. Moreover, the earlier obtained data, including numerical calculations of [6], show that regularity (30), which involves the layer of material entrained from the surface, does not depend on the thermal efficiency of the material, i.e., on the degree of realization of the thermal effect of surface processes and the effect of injection. All of this allows consideration of the possibility of obtaining an expression for calculation of the rate of material entrainment that takes into account only the heat content of the entrained layer.

Interrelation between the Constant of Thermal Destruction and Heat of Material Evaporation. We consider dependence (12) for calculation of the time τ_d obtained on the basis of the constant K_{T_d} from the model of nonstationary heating and entrainment of mass [13] and the formula for determining the same time that follows from the solution of the heat-conduction equation at constant heat flux q = const [6]:

$$\tau_d = \frac{\pi}{4}\lambda\rho c\,\frac{(T_d - T_0)^2}{q^2} . \tag{36}$$

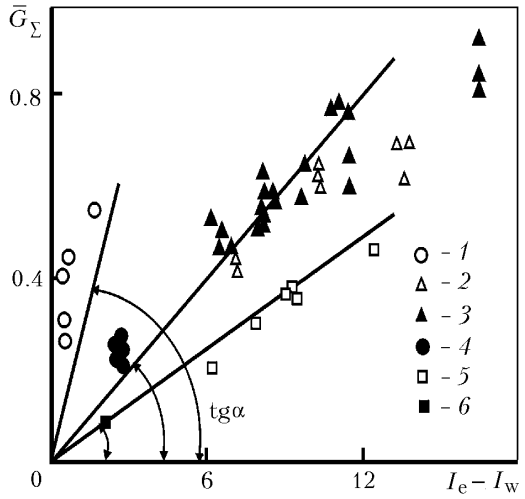

Fig. 11. Dependence of dimensionless rate of entrainment of heat-protective materials on the enthalpy difference in the boundary layer: 1) fluoroplast [25]; 2–4) glass plastic with epoxy binder [2) air plasma; 3) nitrogen plasma; 4) gas generator]; 5, 6) doped quartz-glass ceramic [5) air plasma; 6) gas generator]; straight lines — calculation by (38); tan $\alpha \approx 2(\Delta Q_w)_{max}$. $(I_e - I_w)$, kJ/kg.

In our case, the constant heat flux in formula (36) can be replaced by the integral-mean flow q'_{mean} in time of heating from 0 to τ_T and T_d by the stationary value of the surface temperature $\bar{T}_w$. Having equated formulas (12) and (36), we come to the equation

$$G_\Sigma = \frac{K_{T_d}^3}{(K_{T_d}^2 + 1)\sqrt{\pi}} \frac{q'_{mean}}{c_p(\bar{T}_w - T_0)} \approx \frac{q'_{mean}}{6.8\, c_p(\bar{T}_w - T_0)}. \quad (37)$$

If we consider the maximum heat content of the material $H(T_{boil})$ (at the temperature of boiling), the expression for determining the dimensionless rate of mass entrainment, with account for (35), takes on the form

$$\bar{G}_\Sigma \approx \frac{I_e - I_w}{6.8H(T_{boil})}. \quad (38)$$

Figure 11 presents the dependence of the dimensionless rate of entrainment of fluoroplast, epoxy-binder-based glass-reinforced plastic, and doped quartz-glass ceramic on $(I_e - I_w)$, from which it follows that in the absence of combustion on the surface (the data for fluoroplast are obtained in the flow of nitrogen [25]) and erosion entrainment to the dimensionless rate $\bar{G}_\Sigma < 0.5$ the experimental results [23, 25, 26] are satisfactorily described by Eq. (38). For silica-filler-based glass-reinforced plastic and quartz-glass ceramic at atmospheric pressure, T_{boil} = 3050 K and for fluoroplast $T_{boil} = T_d$ = 1000 K [6]. In this case, the tangent of the angle of slope of linear dependences $\bar{G}_\Sigma \approx f(I_e - I_w)$ turned out to be approximately equal to a double maximum thermal effect of surface processes, which was calculated in [6] for the materials considered.

The possibility of replacing all components of the heat-balance equation in Eq. (38) by the heat content of the material at the limiting temperature, which can still characterize its solid or liquid state, leads to the necessity of considering the interrelation between the heat content and the heat of evaporation of the material [26]. However, as applied to compounds, the data on the heat of evaporation carry less physical information than in the case of simple substances. Moreover, at present the highest accuracy of determination of thermodynamic characteristics is reached for them [27].

We present the interrelation between heat content and heat of evaporation of a substance in the form

TABLE 3. Comparison of the Literature Data on the Thermal Effect of Evaporation of Some Substance with Calculation by Formula (39)

Substance	T_{melt}, K	T_{boil}, K	$\frac{\bar{c}_p}{c_p^{liq}}$, $\frac{kJ}{kg \cdot K}$	ΔQ_{ev}, kJ/kg	
	literature data				calculation by (39)
1	2	3	4	5	6
Ar	83.86 [28], 83.78 [29]	87.29 [28, 29]	$\frac{0.589\ [29]}{0.986\ [28]}$	163.2 [29]	179.5
Kr	115.96 [29], 115.76 [28]	119.96 [29], 119.78 [28]	$\frac{0.245\ [29]}{\sim 0.34\ [29}$	107.7 [29], 107.9 [28]	101.2
Xe	161.3 [28, 29]	165.06 [29]	$\frac{0.2\ [29]}{\sim 0.26\ [29]}$	96.27 [29], 96.05 [28]	113.0
Hg	234.3 [28, 29]	629.89 [29], 630.11 [28]	$\frac{0.119\ [29]}{0.139\ [29]}$	294.7 [29], 294.9 [28]	281.8
Ga	303.0 [30, 31]	2700 [30], 2500 [29]	$\frac{0.27\ [31]}{0.386\ [31]}$	3643 [29]	3424
Rb	312.0 [30, 31]	952 [30] 974 [29]	$\frac{0.298\ [31]}{0.366\ [28]}$	887 [30], 809.5 [29]	1113
K	336.4 [28–30], 336.86 [31]	1052 [30], 1032.2 [28], 1027 [29]	$\frac{0.629[29,31]}{0.746[31]}$	2022 [30], 1982 [29], 1920 [28]	2536
Na	371 [28–30], 371.01 [31]	1187 [30], 1163 [29], 1156 [28]	$\frac{0.93\ [29]}{1.287\ [28]}$	4260 [30], 3873 [29]	4744
In	430 [29, 30, 31]	2440 [29, 30], 2348 [28]	$\frac{0.209\ [31]}{0.238\ [31]}$	1968 [29] 1962 [30]	1931
Li	459 [30], 454 [28, 29], 453.69 [31]	1640 [30], 1590 [29], 1600 [28]	$\frac{2.80\ [29, 31]}{4.21\ [30, 31]}$	19595 [30], 21343 [29], 19412 [28]	21274
Sn	505 [29, 30, 31]	2960 [29], 2473 [30]	$\frac{0.206\ [31]}{0.244\ [31]}$	2447 [29], 2388 [32]	2390
Bi	544 [29, 30]	1900 [30], 1831 [29]	$\frac{0.117\ [29, 30]}{0.15\ [29, 30]}$	823 [30], 725 [29]	908
Tl	577 [29, 30, 31]	1730 [29, 30]	$\frac{0.128\ [31]}{0.142\ [31]}$	795 [29, 30]	808
Cd	594 [29, 30]	1040 [30], 1038 [29]	$\frac{0.217\ [29, 30]}{0.264\ [30]}$	889 [29, 30]	839
Pb	600.6	2023 [30], 2024 [29]	$\frac{0.125\ [29, 30]}{0.137\ [30]}$	858 [30], 866 [29], 842 [32]	918
Zn	693 [29, 30, 32]	1180 [29, 30], 1179 [32]	$\frac{0.366\ [29]}{0.48\ [29, 30]}$	1755 [29], 1754 [30], 1781 [32]	1657
Te	723 [29, 30]	1263 [29], 1360 [30]	$\frac{0.192\ [29]}{0.295\ [30]}$	894 [29], 890 [30]	1014
Mg	923 [29, 30]	1393 [29, 30]	$\frac{1.01\ [29, 30]}{1.378\ [30]}$	5427 [30], 5421 [29], 5514 [32]	5372
Al	933.6 [31], 931.7 [30]	2720 [29], 2600 [30]	$\frac{0.901\ [31]}{1.174\ [31]}$	10885 [29], 10536 [30]	9994
Ba	977 [30], 983 [29]	1911 [30], 1910 [29]	$\frac{0.173\ [30]}{0.225\ [30]}$	1087 [30], 1099 [29]	1289
Sr	1043 [29, 30]	1657 [30], 1640 [29]	$\frac{0.28\ [30]}{0.367\ [30]}$	1606 [30], 1585 [29]	1759
Ca	1115 [31], 1123 [30]	1755 [30], 1760 [29]	$\frac{0.751\ [31]}{0.776\ [31]}$	4032 [30], 3743 [29]	4536
La	1193 [28, 31], 1153 [30]	3643 [29], 3000 [30]	$\frac{0.226\ [31]}{0.236\ [31]}$	2880 [29], 2412 [30], 2892 [33]	2882
Ge	1232 [30], 1210 [29]	2980 [30], 3101 [29], 3125 [33]	$\frac{0.347\ [29, 30]}{0.422\ [30]}$	3931 [30], 4601 [29]	3961

TABLE 3 Continued

1	2	3	4	5	6
Ag	1234 [29, 30]	2485 [29, 30]	0.237 [29, 34] / 0.319 [34]	2357 [30], 2354 [29]	2351
Au	1336 [29, 30], 1337 [34]	2933 [30], 2800 [34], 2973 [29]	0.135 [29, 30] / 0.149 [29, 30]	1577 [30], 1647 [29]	1422
Cu	1356 [29, 30]	868 [29, 30], 2630 [32]	0.398 [29, 30] / 0.494 [29, 30]	4797 [30], 4784 [29], 3596 [32]	4374
Be	1560 [31], 1556 [29]	2750 [29], 2720 [33]	2.485 [31] / 3.354 [31]	32622 [29]	26750
Si	1683 [30], 1696 [29]	2750 [30], 2628 [29]	1.04 [29, 30] / 1.104 [30]	10575 [30], 14046 [29]	9956
Ni	1728 [30], 1726 [29]	3110 [30], 3073 [29]	0.499 [29, 30] / 0.656 [30]	6453 [30], 6483 [29], 6475 [35]	6014
Co	1766 [30], 1765 [29]	3370 [30], 2528 [29]	0.54 [29, 30] / 0.59 [30]	6600 [30], 6499 [29]	6460
Y	1801 [31], 1750 [30], 1773 [29]	3473 [29], 3500 [30], 3610 [33]	0.367 [31] / 0.445 [31]	4420 [29], 4245 [31]	4777
Fe	1808 [29, 20]	3043 [30]	0.578 [29, 30] / 0.75 [30]	6805 [30]	6702
Sc	1814 [31], 1670 [29, 30]	3000 [30], 2970 [33]	0.73 [31] / 0.979 [31]	7452 [30], 6782 [29]	8450
Pd	1824 [30], 1825 [29, 34]	3440 [30], 3833 [29], 4253 [34]	0.266 [29, 30] / 9.354 [30]	3505 [30], 4182 [43]	3595
Ti	1944 [31], 1941 [29], 2000 [30]	3550 [29, 30], 3550 [33]	0.66 [31] / 0.975 31]	8977 [29], 8829 [30], 9841 [33]	9683
Th	2023 [31], 1968 [29]	4470 [29], 4500 [30]	0.198 [31] / 0.144 [31]	2344 [29], 2346 [30]	2633
Pt	2042 [29, 34]	4580 [29], 4800 [34]	0.149 [29, 30] / 0.193 [30]	2620 [30], 2660 [34]	2700
Zr	2125 [30], 2128 [29]	3900 [30], 4653 [29]	0.317 [29, 30] / 0.367 [30]	4582 [30], 6380 [29]	4505
Cr	2176 [29], 2173 [30]	2915 [29], 2495 [30], 2700 [33]	0.61 [29, 30] / 0.754 [30]	6712 [29], 5875 [30]	6414
V	2220 [31], 2003 [29]	3653 [29], 3582 [33], 3800 [30]	0.599 [31] / 0.907 [31]	8990 [29], 9010 [33]	8937
Rh	2239 [34], 2233 [29], 2240 [30]	4770 [34], 4233 [29], 4150 [30]	0.309 [29, 30] / 0.366 [30]	5620 [34], 5167 [30]	5502
Hf	2506 [31], 2493 [29]	5473 [29], 5670 [33]	0.188 [31] / 0.244 [31]	3703 [29]	4060
Ir	2716 [34], 2727 [30]	5570 [34], 4623 [29]	0.159 [29, 33] / ~0.205 [30]	3310 [34]	3457
Nb	2750 [31], 2760 [30]	5400 [33], 5173 [29]	0.323 [31] / 0.45 [31]	7667 [33], 7491 [29]	7076
Mo	2896 [31], 2898 [29], 2883 [30]	5100 [33], 5073 [29]	0.334 [31] / 0.416 [31]	6800 [33], 6191 [29], 7400 [35]	6409
Ta	3295 [31], 3269 [29], 3250 [30]	5673 [29], 5570 [33]	0.167 [31] / 0.248 [31]	4161 [29], 4168 [33]	3883
Os	3320 [34], 2940 [30]	5770 [34]	0.168 [29, 33] / ~0.196[30]	3561 [34]	3479
W	3695 [31], 3653 [29]	5800 [29], 6170 [33]	0.175 [31] / 0.1245 [31]	4346 [29], 4957 [33]	3952
SiO_2	1996 [31]	2770 [35]	1.058 [31] / 1.443 [31]	12 000 [6]	10976

$$\Delta Q_{\text{ev}} \approx \frac{(K_{T_\text{d}}^2 + 1)\sqrt{\pi}}{2K_{T_\text{d}}^3} H(T_{\text{boil}}) \approx 3.4H(T_{\text{boil}}), \quad (39)$$

where $H(T_{\text{boil}}) = \bar{c}_p T_{\text{melt}} + c_p^{\text{liq}}(T_{\text{boil}} - T_{\text{melt}})$. In this expression, the heat content of a substance heated to the temperature of boiling must be considered separately for the liquid and solid states. Since for most substances heat capacity in the molten state changes slightly, it was, for the most part, taken constant. However, for the solid state we must take into account the dependence of heat capacity on temperature and in calculation take its integral-mean value within the range of temperatures from 0 to T_{melt}.

From the analysis of the literature data given in Table 3 we found that, actually, the thermal effect of evaporation of most simple substances with an accuracy up to 7% can be calculated by formula (39). Here, we must pay attention to the fact that the more accurately the temperatures of melting and boiling and heat capacities of the substance in the solid and liquid states are determined, the better the agreement of the literature and calculated data (for example, for silver this agreement is complete).

Thus, the physical meaning of the constant of thermal destruction lies in the fact that in dimensionless form it characterizes the amount of heat (energy) that must be absorbed in the surface layer of the material for transition from the nonstationary mode of mass entrainment to the stationary one, including the case of erosion destruction of the material surface. Allowing for the relation between K_{T_d} and the heat of evaporation, we can speak of some analogy between this process and the thermal effect necessary for breaking the bonds in transition from one aggregate state of a substance to another.

Temperature Field near the Material Surface. Establishment of the Stationary Mode of Destruction. The results obtained are beyond the scope of the theoretical concept of material ablation in the high-temperature flow. The reason for this is probably in the origination of a special "zone" with an anomalous mechanism of absorption and transfer of heat near the destructing surface of the material, which, to some extent, must reflect on the temperature field. To elucidate this problem, we studied temperature fields in quartz-glass ceramic. The technique and some results of these experiments are given in [12].

It is assumed that the S-shaped profile can appear only in the case of radiative heat transfer, i.e., with sharp increase in the thermal conductivity of the material due to the radiative component of heat transfer. Therefore, to determine the degree of transparency of quartz-glass ceramic specimens, we conducted spectrophotometric measurements which showed that light transmission in quartz-glass ceramic doped by chromium oxide is only ~0.05%. Moreover, in [10, 11] it was shown that at a temperature of ~1800 K in this ceramic, in contrast to pure quartz-glass ceramic, a sharp boundary is formed, above which the material is virtually nontransparent.

Figure 12 presents the temperature profiles in the specimens of pure and doped quartz-glass ceramic in the quasistationary mode of heating and entrainment of mass of these materials. They are in full correspondence with the theoretical models. The S-shaped profile in the near-surface layer of pure ceramic is in good agreement with calculation by (1)–(3), which is explained by the fact that its thermal conductivity at temperatures higher than 2000 K increases threefold as compared with the thermal conductivity of doped ceramic (Fig. 13). As should be expected in doped ceramic, whose thermal conductivity increases weakly with temperature, the temperature profile in the quasistationary mode of heating is of an exponential character.

However, it turned out that in the nonstationary mode of heating, the S-shaped temperature profile is also observed in the specimens of nontransparent quartz-glass ceramic (Fig. 14). In the nonstationary mode of heating of doped quartz-glass ceramic this profile remained up to the establishment of the quasistationary mode.

From the viewpoint of the existing concepts, one of the explanations of this result can be the following: from the moment of the onset of destruction (melting) of the quartz-glass ceramic surface some amount of heat is spent for the breaking of bonds. In the case of crystal material it is larger, whereas for glassy material it is smaller. This can lead to slowing down of the increase in the surface temperature, which is specified by the heat flux before surface destruction, and, correspondingly, to deformation of the temperature profile. However, the drawback of this explanation is that the heat of melting of amorphous silicon dioxide is 128 kJ/kg, i.e., just higher than 5% of its heat content at the temperature of melting (2140 kJ/kg), and can hardly lead to such a great bend of the temperature profile, the more so that in the quasistationary mode of heating of doped (nontransparent) quartz-glass ceramic the S-shaped profile dis-

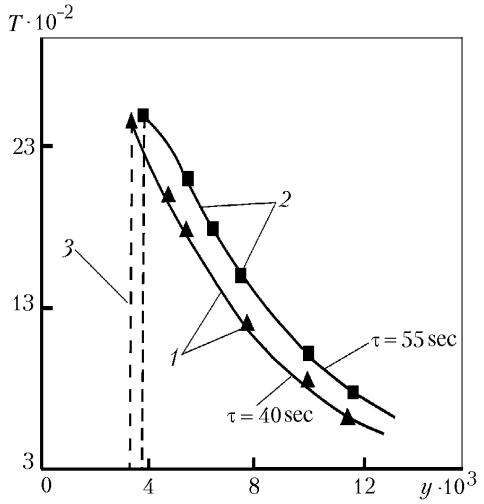

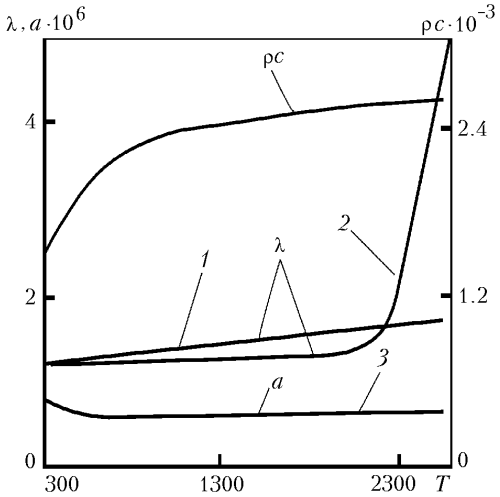

Fig. 12. Comparison of temperature profiles in pure and doped quartz-glass ceramic: 1) doped quartz-glass ceramic at the 40th second of heating (q_{cal} = 8350 kW/m^2, T_w = 2390 K, $\bar{V}_\infty = 0.1\cdot10^{-3}$ m/sec); 2) pure quartz-glass ceramic at the 55th second of heating (q_{cal} = 7260 kW/m^2, T_w = 2510 K, $\bar{V}_\infty = 0.08\cdot10^{-3}$ m/sec); 3) position of the heated surface; dots — experiment; curves — calculation by (1)–(3). T, K; y, m.

Fig. 13. Thermophysical characteristics of quartz-glass ceramic: 1, 3) doped; 2) pure. λ, W/(m·K); ρc, kJ/(m^3·K); a, m^2/sec; T, K.

appears completely (see Figs. 12 and 14). At the same time, if, as has been shown, not less than 1000 kJ/m^2 are absorbed in the surface layer of the material before the establishment of the stationary mode of mass entrainment, the revealed bend of the temperature profile is quite possible. Probably, the mechanism of attainment of the stationary mode of mass entrainment is similar to erosion destruction [20, 21].

It was mentioned above that numerical calculations by the existing models of heating and mass entrainment [6] allow one to confirm the found regularities only for the in-depth isotherms and are not in agreement with the experimental data obtained at high temperatures. At the same time, it was shown that there exist two instants of time when calculation by formulas (22) and (36) obtained on the basis of the "classical" heat-conduction theory is in good agreement with calculation by the equations of the experimental model of heating and mass entrainment that includes the constant of thermal destruction (12) and (27), i.e., two absolutely different approaches are in good correspondence with each other at the beginning and end of the nonstationary mode of heating with mass entrainment.

According to the experimental model of heating and mass entrainment that includes the constant of thermal destruction, the rate of entrainment is specified by the heat flux even before the onset of surface destruction and is established at the moment when a layer of certain thickness ($S(\tau_v) = d_0/K_{T_d}$), which depends on the thermal conductivity of the material, is entrained from the surface. However, as soon as the stationary rate is established, the thermal conductivity of the material affects the rate of entrainment by no means. Further, its variation will be determined only by the heat balance on the destructing surface of the material. This conclusion is in agreement with formula (3), although it is obtained by the model supporting the establishment of the stationary mode of mass entrainment in infinite time of heating [6].

Hence it follows that with sufficient thermal load the stationary mode of mass entrainment does not require an infinite time of heating to be established. Entering of heat to the inner layers of the material stops depending on its thermal conductivity and is determined only by the velocity of movement of the surface from the moment of termination of the process of heat accumulation in the surface layer, the amount of which is determined by the constant $\underline{K}_{T_d}$. Precisely at this moment we can assume that the temperature profile, if the isotherms with temperature close to $\bar{T}_w$ are considered, became stationary, since the velocity of the isotherms became equal to the rate of entrainment. The model suggested (see Fig. 9) assumes full coincidence of the current temperature profile with the stationary one upon transition to the isotherm with a lower temperature, rather than gradually approaching it. It is seen from Fig. 14 that

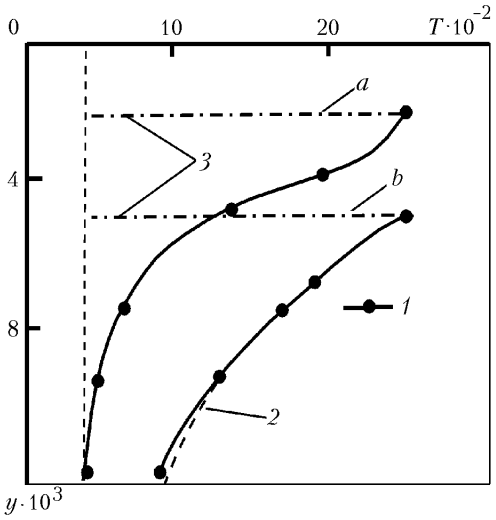

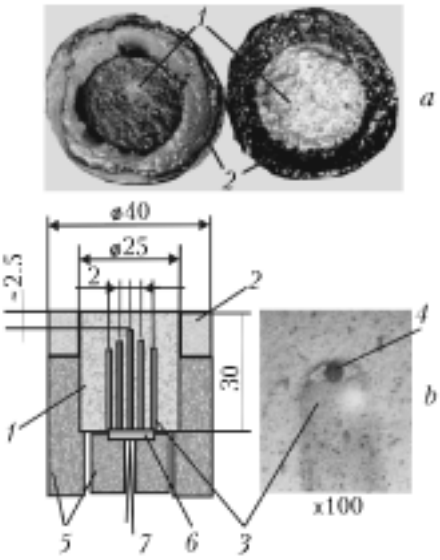

Fig. 14. Experimental temperature profiles in the specimen of doped quartz-glass ceramic at $\bar{V}_\infty = 0.11\cdot10^{-3}$ m/sec: 1) experiment; 2) stationary temperature profile; 3) position of the heated surface ($q_{calc} = 7260$ kW/m^2); a) at the 15th second of heating; b) at the 50th second of heating. T, K; y, m.

Fig. 15. External appearance of the specimens of doped quartz-glass ceramic after testing (a) and the schematic of the arrangement of thermocouples in the specimen (b): 1) specimen; 2) ceramic (protective) ring made of quartz-glass ceramic; 3) ceramic plate made of quartz-glass ceramic; 4) thermocouple; 5) asbestos bushings; 6) copper plate; 7) controlling thermocouple.

at the 50th second of heating the experimental profile for doped quartz-glass ceramic fully coincides with that calculated for the stationary mode, and only for the isotherms with low temperature is the deviation from the stationary profile determined by the equation obtained in [6] observed:

$$\theta(y) = \frac{T(y) - T_0}{\bar{T}_w - T_0} = \exp\left(-\frac{\bar{V}_\infty}{a} y\right). \tag{40}$$

It is just this sense in which the mode of heating remains stationary.

To measure temperatures in quartz-glass ceramic specimens, in the experiments we have taken necessary precautions to avoid side heating (Fig. 15a) and checked the possibility of material shrinkage by measuring the coordinates of the thermocouples on the specimens cut after the tests (Fig. 15b).

Thus, the regularities found, including the linear dependence $\Delta^* = f(\sqrt{\tau})$ for high-temperature isotherms, are a consequence of one phenomenon — the S-shaped temperature profile or the "zone" near the destructing surface of the material.

Nevertheless, calculations of the entrainment of mass of the heat-protective material by the heat-conduction equation (21), which, in fact, does not allow for the established mechanism of heat absorption in the surface layer, and by Eqs. (16), (17), and (20) obtained on the basis of the constant of thermal destruction are in satisfactory agreement even under variable thermal effect (see Fig. 3). This can be explained as follows. First, the governing influence of the rate of heat supply on the rate of heating and mass entrainment even before the onset of destruction of the material surface was found; it was also revealed that the processes occurring both on the surface and close to it weakly affect the temperature field inside the material. In those modes of thermal effect when the heat content of the material forms a noticeable part in the heat balance, the velocity of movement of the depth isotherms ($\theta^* \le 0.1$) greatly exceeds the rate of mass entrainment, and numerical calculations of [6] also show that for these isotherms regularity (30) holds

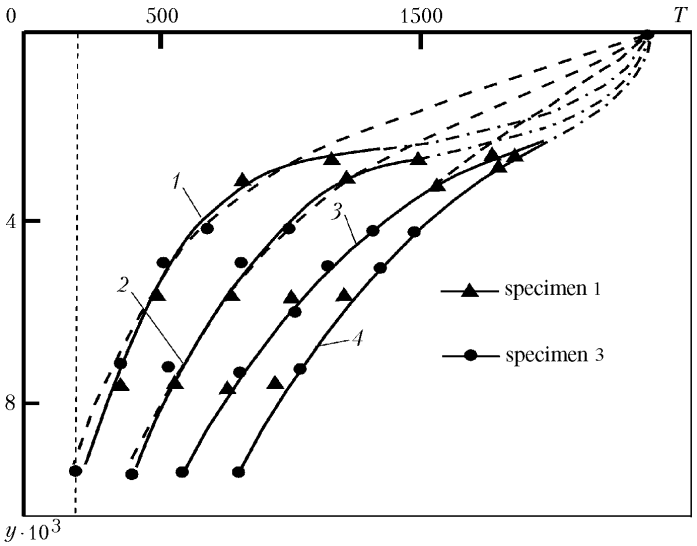

Fig. 16. Temperature profiles obtained in specimens 1 and 3 of doped quartz-glass ceramic in melting of the surface without mass entrainment: 1–4) time of heating 10, 20, 40, and 60 sec; dots and solid curves — experiment; dashed lines — calculation by (7); dash-dot lines — assumed temperature profile near the heating surface. *T*, K; *y*, m.

with an accuracy up to 10%. Second, the values of the rate of entrainment that are calculated by the model of quartz glass fusion with account for viscosity [6] and are presented in the form of (18) at $\Delta\varepsilon = 10\%$ also determine the value of K_{T_d} with satisfactory accuracy.

Temperature Field near the Destructing Surface of a Material without Mass Entrainment. Although most high-temperature processes, for example, welding, cutting, electric slag remelting, etc., occur at temperatures that exceed the temperature of melting of the material processed, they (except for cutting) do not lead to considerable entrainment of material mass and in these cases the use of the regularities found in investigations of ablating heat-protective coatings requires additional verification. Here, it is also of interest to find which processes occur in the surface layers of the material in melting of its surface without mass entrainment.

To answer this question, we conducted a computational-experimental study of movement of the isotherms in formation of melt on the surface of the samples of doped quartz-glass ceramic virtually without entrainment of the melt film [36]. The technique of the experiments on measurement of temperature fields in the specimens of quartz-glass ceramic is described in [12]. However, setting-up of this investigation required the provision of melt-retention on the specimen surface. For this purpose it was necessary to select a corresponding mode of operation of the electric-arc heater developed at the A. V. Luikov Heat and Mass Transfer Institute of the BSSR Academy of Sciences [25] and to cover the side surface of the specimen with a material which by its thermophysical characteristics and heat resistance is as good as the specimen material. Therefore, to protect the side surface of the specimens we manufactured ceramic rings made of quartz-glass ceramic. The material for the rings was selected so that the color of their surface after melting differed from the color of the specimen studied, which can easily be provided by a slight change in the content of the doping additive Cr_2O_3. This made it possible to convince ourselves in the absence of entrainment of the material from the specimen surface in the form of the melt film (Fig. 15a). The experiments were conducted in a subsonic air-plasma jet at heat flux of 2500 kW/m^2. The stagnation enthalpy amounted to about 4500 kJ/kg and the surface temperature of the specimens changed within 2300–2450 K. The diameter of the ceramic ring was selected so that uniform distribution of the heat flux over the entire surface of heating, including the ring surface, can be provided. The schematic of arrangement of tungsten–rhenium thermocouples (the thermoelectrode diameter is 0.1 mm) in the specimen and the outer appearance of the thermocouple inside it after tests are shown in Fig. 15b. Since the stagnation enthalpy of the oncoming air flow at which the experiment was conducted was ~4500 kJ/kg (corresponds to the coefficient of gasification ≤0.1 [23, 24]), mass entrainment due to evaporation is negligible. Values of temperatures meas-

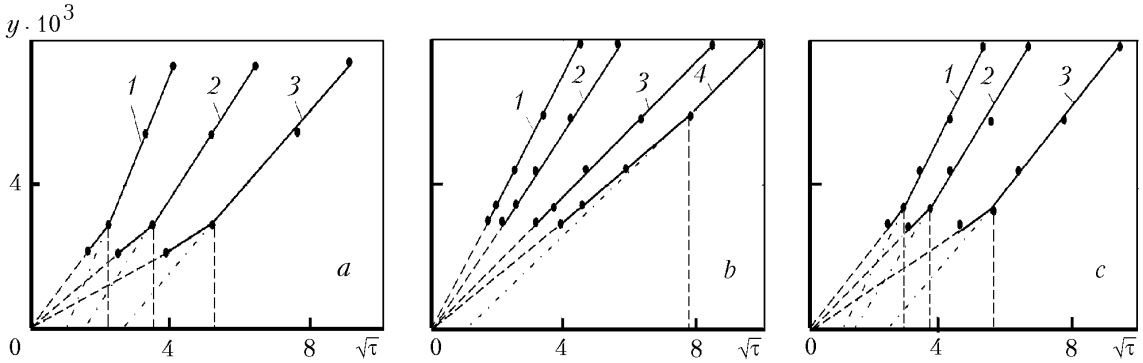

Fig. 17. Dependences of movement of isotherms in the specimens of doped quartz-glass ceramic on the square root of the time of heating in melting of the surface without mass entrainment: a) specimen 1 [1–3) $\theta^* = 0.1$, 0.3 and 0.5]; b) specimen 2 [1–4) $\theta^* = 0.1$, 0.2, 0.4, and 0.5]; c) specimen 4 [1–3) $\theta^* = 0.1$, 0.2, and 0.4], dashed lines — calculation by (7) at $\bar{T}_w$ = const; dash-dot lines — approximation of linear dependences $y = f(\sqrt{\tau})$ for determination of time τ_ξ. y, m; $\sqrt{\tau}$, $\text{sec}^{0.5}$.

TABLE 4. Results of Testing of the Specimens of Quartz-Glass Ceramic in Melting of the Surface without Mass Entrainment [1) experiment; 2) calculation by (41)] (q_{cal} = 2500 kW/m^2)

Specimen No.	$a \cdot 10^6$, m^2/sec	λ, W/(m·K)	T_w, K	τ_d, sec	τ_T, sec	
					1	2
1	0.5	1.26	2350	1.15	14.0	11.0
2	0.65	1.64	2300	1.5	14.0	16.2
3	0.5	1.26	2320	1.15	14.0	12.3
4	0.45	1.13	2450	1.04	8.0	7.4

ured by the tungsten–rhenium thermocouples reached ~1900 K. The depth of the arrangement of the thermocouples was verified on the cut specimens after the tests.

The time of establishment of the surface temperature was estimated by a formula obtained in [19], which involves the constant K_{T_d}:

$$\tau_T \approx \left[\frac{560}{K_{T_d} (\bar{T}_w - T_d)} + \sqrt{\tau_d} \right]^2 . \qquad (41)$$

To calculate the time of reaching the temperature of onset of melting of the material surface τ_d, we used formula (36). The temperature of the beginning of quartz-glass ceramic melting T_d was taken equal to 2000 K [10]. Thermal diffusivity was determined directly from the obtained temperature fields by comparing calculated and experimental values of temperatures; here we took ρc = 2520 kJ/m^3 (see Fig. 13).

First of all, we should mention the good duplication of the results obtained. Figure 16 presents the temperature profiles in specimens 1 and 3 (Table 4), which have the same thermal diffusivity and close values of the surface temperature (2350 and 2320 K). It is seen from the figure that the temperature fields in these specimens are in rather satisfactory agreement. Since in all the cases considered τ_T did not exceed 14 sec (the time of experiments was 100–120 sec), this allowed us to compare the experimentally obtained temperature fields with calculation by formula (7) obtained at T_w = const.

Comparison of calculated and experimental data shows that in all the cases considered the isotherms with dimensionless temperature $\theta^* \le 0.4$ are in satisfactory agreement with the experimental results with calculation by formula (7) obtained for the "classical" self-similar mode at T_w = const. Earlier it was shown that termination of the

process of heat accumulation in the surface layer of the material is especially noticeably reflected in the regularity of movement of high-temperature isotherms — the angle of inclination of the straight lines $\Delta^* = f(\sqrt{\tau})$ changes (see Figs. 4 and 5). In surface melting without mass entrainment we observe a substantial bend of the linear dependences of the path $y = K\sqrt{a\tau}$ passed by the isotherms. However, in contrast to heating with mass entrainment, after a change in the angle of inclination these dependences have no common "focus" (Fig. 17).

It is shown in Fig. 17a and b that the time of heating in which the angle of inclination changes strongly depends on the thermal diffusivity of the specimen. If for specimen 1, the thermal diffusivity of which was 25% smaller than that of specimen 2 (Table 4), the angle of inclination of the dependence $y = K\sqrt{a\tau}$ for $\theta^* = 0.1$ changes at the 5th second of heating (Fig. 17a), in specimen 2 this occurs only for the isotherm $\theta^* = 0.5$ at the 60th second of heating (Fig. 17b). The time of variation of the angle of inclination is also affected by the surface temperature. For example, despite the fact that the coefficient a for specimen 4 (T_w = 2450 K) was somewhat lower than for specimen 1 (Table 4), the angle of inclination for the dependence of the path passed by the isotherm $\theta^* = 0.1$ changes about 3 sec later (Fig. 17c) than for specimen 1 (T_w = 2350 K). Thus, the farther the considered isotherm can succeed into "running" from the heating surface, the smaller its influence on the latter. In melting without mass entrainment, the temperature field, when $\theta^* > 0.4$–0.5, no longer satisfies the self-similar solution of (7) (see Fig. 16, dashed curves) and the linear dependence $y = f(\sqrt{\tau})$ ceases to exist.

Based on the results given in Figs. 4, 5, and 17, we can draw the conclusion that the higher the temperature of the isotherm under consideration, the higher the effect of the processes near the destructing surface on the character of movement of the isotherms, i.e., the reason for the change in the angle of inclination of linear dependences ($y = f(\sqrt{\tau})$ or $\Delta^* = f(\sqrt{\tau})$) is formation of some "zone" near the surface of the destructing material. The temperature profile is strongly deformed near the surface and it acquires the S-shaped form (see Figs. 14 and 16).

It should be emphasized that the "zone" with anomalous conditions of heat transfer near the destructing surface exerts a great effect on nonstationary heating and entrainment of mass of only those materials whose thermal conductivity is low, including ablating heat-protective coatings. Since with an increase in thermal conductivity of the material the effect of the "zone" on the temperature field decreases strongly, in calculation of the heating of, for example, metals and alloys its influence can be neglected even at high temperatures.

It is of interest to note that determination of the interface slag–metal in electric slag remelting is based on considerable increase in the value of heat flux on the wall in this zone. Although this method of control has long been used, the reason due to which heat flux increases has not yet been explained satisfactorily [37].

Limiting Energy Capacity of Surface Processes of Heat Absorption. At the rate of mass entrainment exceeding $\overline{G}_\Sigma \geq 0.5$, the contribution of the heat content of the material sharply decreases as compared to the heat absorbed due to physicochemical conversions on the surface and the effect of injection. Under these conditions, the time of existence of the linear dependences $\Delta^* = f(\sqrt{\tau})$ is too small, the inner processes of heat absorption can be neglected, and expression (38) cannot be used. Since, according to (4), the rate of entrainment depends on many parameters, $\overline{G}_\Sigma = f(I_e)$, as should be expected, has a rather complex character. However, in [38, 39] it is shown that the results of the experimental studies of materials of different classes and numerical calculations of mass entrainment of quartz glass within the range I_e = 10,000–50,000 kJ/kg and $P_e = 10^4$–10^7 Pa can be presented as

$$\overline{G}'_\Sigma \approx \sqrt{\frac{I_e - I_w}{H}} - 0.3 . \qquad (42)$$

Here $\overline{G}'_\Sigma = \overline{G}_\Sigma (I_e - I_w)/(I_e - I_0)$, i.e., the dimensionless rate of entrainment is considered relative to the initial drop of enthalpy or heat flux onto the cold surface.

Moreover, processing of the experimental data given in [39–41] by the least-squares method showed that the normalizing factor H in formula (42) as well as in Eq. (38) is approximately equal to double the maximum thermal effect of surface processes and the "focus" is of about 0.3 (Fig. 18). In this case, by $(\Delta Q_w)_{max}$ for fluoroplast we mean the heat of decomposition, for glass-fiber-reinforced plastic and quartz-glass ceramic — the total thermal effect of physicochemical conversions at the temperature of boiling, and for graphite — the maximum value of sublimation heat. In calculation of $\overline{G}'_\Sigma$ within the range $0.4 < \gamma\overline{G}_w < 1.2$, Eq. (4) was transformed with account for the corresponding approximation for the effect of injection [6].

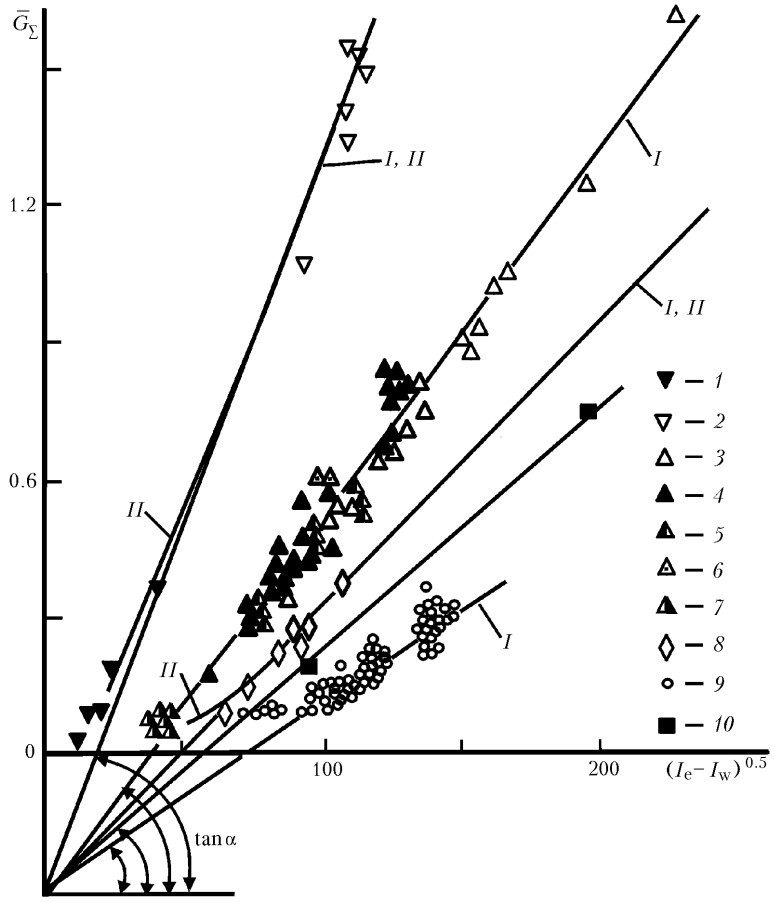

Fig. 18. Dependence of dimensionless rate of entrainment $\bar{G}'_\Sigma$ on the enthalpy difference: 1, 2) fluoroplast [1) argon; 2) nitrogen; $P_e = 1 \cdot 10^5$ Pa] [25]; 3–7) glass plastic with epoxy binder [3) air, $P_e = 1 \cdot 10^5$ Pa [41], 4) air, $P_e = 1 \cdot 10^5$ Pa [39], 5) nitrogen, $P_e = 1 \cdot 10^5$ Pa [39], 6) air, $P_e = 0.3 \cdot 10^5$ Pa [39], 7) products of combination of "kerosene–oxygen" fuel, $P_e = 3.5 \cdot 10^5$ Pa [39]]; 8) doped quartz-glass ceramic (air, $P_e = 1 \cdot 10^5$ Pa) [39]; 9) graphite (air, $P_e = (0.3–4.2) \cdot 10^5$ Pa [40]; 10) carbon plastic (air, $P_e = 1 \cdot 10^5$ Pa) [39]; I — calculation by (42), II — calculation by (4); $\tan \alpha \approx [2(\Delta Q_w)_{max}]^{-0.5}$, $(kJ/kg)^{0.5}$.

Results of the experimental investigations and numerical calculations by the model of fusion of quartz glass with account for viscosity showed that regularity (42) holds within a wide range of thermogasdynamic parameters. However, it is known that the coefficient of injection γ in the turbulent mode of flow is 2–3 times smaller than in the laminar mode [6]. Moreover, the thermal pattern of the process of destruction of a streamlined body can be complicated by erosion entrainment, semi-transparency of the material, combustion, and different technological factors. All these effects, to a greater or lesser extent, must lead to an increase in the actual rate of mass entrainment [42].

To prove the generality of regularity [42] and determine the limits of its applicability, in [42] we considered the conditions of stabilization of the parameters of thermal destruction of materials. As the flow enthalpy increases, the difference in chemical individuality of the destruction models becomes smaller, whereas the influence of the effect of injection in the heat balance becomes more substantial [43]. The role of melt viscosity also decreased, and most materials are carried away, as a rule, in a gaseous form already at a flow enthalpy higher than 20,000 kJ/kg. All of what was stated above gives grounds for construction of a simplified scheme of thermal destruction with a minimum number of determining parameters [44].

At rather high levels of thermal effect we can neglect radiation from the destructing surface and take the parameter of internal heat absorption to be constant, $H^* = H(T_w) + \Delta Q_w = \text{const}$. Then, the heat balance on the destructing surface of the body is written as

$$q_0 = (\alpha / c_p)_0 (I_e - I_w) = \varepsilon\sigma T_w^4 + q_{inj} + G_w [H(T_w) + \Delta Q_w] \approx q_{inj} + G_w H^* . \quad (43)$$

In linear approximation of injection

$$\Psi = \frac{q_w}{q_0} = 1 - \gamma \bar{G}_w \quad (44)$$

heat balance (43) is reduced to the following equation for determining $\gamma\bar{G}_w$ (γ is the injection parameter, which for a laminar boundary layer is 0.6):

$$\gamma \bar{G}_w = \frac{\gamma z}{1 + \gamma z}, \quad (45)$$

where $z = (I_e - I_w)/H^*$.

In [42] it is shown that for square approximation of injection

$$\Psi = \frac{1}{3(\gamma \bar{G}_w)^2 + \gamma \bar{G}_w + 1} \quad (46)$$

the heat balance can be presented in the form

$$\gamma \bar{G}_w = \sqrt[3]{\frac{\gamma z}{3}} \left(1 - \frac{0.2}{\sqrt[3]{(\gamma z)^2}}\right) - \frac{1}{9}. \quad (47)$$

Finally, from (42), by reducing it to a form similar to (45) and (47), with account for (39) we have

$$\gamma \bar{G}_w - \sqrt{\gamma z \left(\frac{\gamma}{1.5}\right)} - 0.3\gamma . \quad (48)$$

Comparison of the experimental data with different-in-accuracy solutions in the form of (45) and (47) and Eq. (48), which was made in [42], indicates the existence of the universal dependence of $\gamma\bar{G}_w$ on γz. Thus, empirical relation (42) can be extended to any other conditions if the coefficient of injection strongly differs from the mean "laminar" value 0.6 and $\gamma z < 5$.

Since in (42) $H \approx 2(\Delta Q_w)_{max}$ should be taken as the parameter of stabilization of entrainment of the material mass, it must depend on both the inner heat absorption of the material $H^* = H(T_w) + \Delta Q_w$ and the effect of injection. Actually, with an accuracy up to 10% we can write $H \approx [H(T_w) + \Delta Q_w]/\gamma$. Then we present (42) in the form

$$\bar{G}_w \approx \sqrt{\frac{\gamma (I_e - I_w)}{\Delta Q_w + H(T_w)}} - \frac{H(T_w)}{\Delta Q_w} = \sqrt{\gamma z} - 0.3 , \quad (49)$$

from which we see that the dimensionless rate of material evaporation is in direct proportion to the square root of the ratio of the main parameters determining heat transfer in the boundary layer and heat-protective capabilities of the material [45]. This equation must hold in injection of fully gasified products of thermal destruction of material into the laminar boundary layer and in an "ideal" heat-protective material for which the maximum thermal effect of physicochemical conversions on the surface exceeds its heat content at the temperature of boiling by 3.4 times. At the present time, to such heat-protective materials we can, likely, refer only doped quartz-glass ceramic, if under the considered

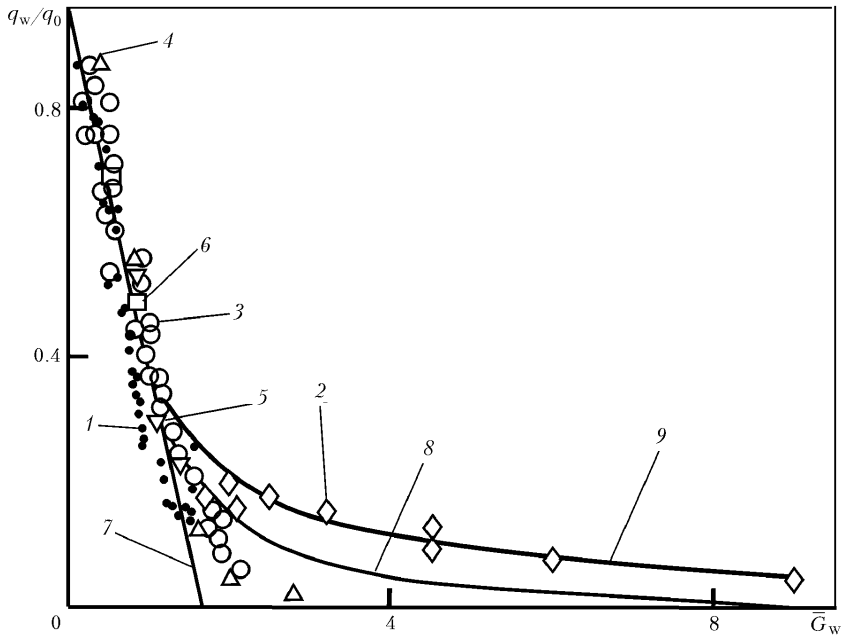

Fig. 19. Influence of $\bar{G}_w$ on the ratio q_w/q_0: 1) [43]; 2) [46]; 3) [47]; 4) [48]; 5) [49]; 6) [50]; 7) calculation by (44); 8) by (46); 9) by (50).

conditions of heating it is taken to be nontransparent, and some carbon–carbon compositions stable to oxidizing and thermomechanical actions of the incoming gas flow.

To verify the validity of expression (49), we obtain a relation for the dimensionless function of heat transfer:

$$\Psi = \frac{q_w}{q_0} = \frac{\bar{G}_w}{z}, \tag{50}$$

which is confirmed by the experimental data of [46] to the values of the dimensionless parameter of injection $\bar{G}_w = 9$ (Fig. 19), whereas, for example, for quartz glass even at an enthalpy of 100,000 kJ/kg, $\bar{G}_w < 2$. Only in entering the atmosphere of Jupiter does the enthalpy of the delayed flow exceed this value [51].

The results obtained make it possible to find the limiting energy capacity of the whole process of thermal destruction of a material. With this in mind, we use the expression for effective enthalpy and regularity (42). Provided that the stagnation enthalpy $I_e \to \infty$, we have

$$I_{eff} = \frac{q_0 - \varepsilon\sigma T_w^4}{G_\Sigma} \to \frac{q_0}{G_\Sigma} = \frac{(\alpha/c_p)_0 (I_e - I_w)}{\left[(\alpha/c_p)_0 \sqrt{\dfrac{(I_e - I_w)}{H}} - 0.3\right]} \to \sqrt{(I_e - I_w) H}\,. \tag{51}$$

In the limit, $I_{eff} \to \sqrt{I_e H}$ when $I_e >> I_w$.

The Constant of Thermal Destruction and the Critical Coefficient of a Substance. By virtue of the fundamental importance of the constant of thermal destruction of a material for the processes of heating and mass entrainment, an attempt was undertaken to explain numerical values of the constant $K_{T_d} = 0.74$ and the coefficient 3.4, which establishes the relation between heat capacity and heat of material evaporation.

According to the data of different authors, for example [52, 53], oxygen and silicon are the most widespread elements in the Earth's crust (O ~ 50%, Si ~ 25–30%). Clearly, the materials based on SiO_2 have gained the widest acceptance. It is of interest to note that within the entire range of temperatures from 2000 to 2730 K the ratio of heat capacities of SiO_2 in the gaseous and liquid states is numerically equal to the value of the constant of thermal destruction $K_{T_d} = 0.74$ [31]. According to Table 3, the heat of evaporation of most simple substances is related to their heat

TABLE 5. Critical Parameters of Some Substances

Substance	T_{cr}, K	$P_{cr}\cdot10^{-5}$, Pa	$V_{cr}\cdot10^{3}$, m^3/kg	Reference	$z_{cr} = \frac{RT_{cr}}{P_{cr}V_{cr}}$
NH_3	405.6	112.9	4.25	[28]	4.12
	405.5	112.8	4.25	[29]	4.12
H_2O	647.28	221.2	3.15	[28]	4.29
	647.3	221.3	3.13	[29]	4.32
Hg	1763	1510	0.182	[28]	2.66
	1460±20	1662±50	0.2–0.24	[29]	1.46–1.9
K	2250	160	6.25	[28]	4.78
	2228±300	162	5.35	[29]	4.73–6.2
Na	2500	370	5.56	[28]	4.4
	2570±350	355	5.05	[29]	4.48–5.9
Li	3800	970	10.0	[28]	4.69
	3200±600	689	9.51	[29]	4.75–6.95
Rb	2100	160	2.86	[28]	4.47
	2093±35	159	2.89	[29]	4.26–4.51
Cs	2050	117	2.33	[28]	4.71
	2057±40	147	2.34	[29]	3.67–3.81

content by the coefficient 3.4 obtained on the basis of the constant. Since the heat content of the material depends on its heat capacity, this gives grounds to assume that the numerical value of K_{T_d} is a consequence of the ratio of heat capacities of SiO_2 in the gaseous and liquid states.

In the first approximation, the coefficient 3.4 can be explained as follows. As pressure increases, the enthalpy of a liquid increases and reaches the maximum at critical pressure and temperature. In turn, the heat of evaporation decreases with an increase in pressure and at the critical pressure it is zero. Comparison of enthalpies of liquid and vapor on the saturation line for individual substances given in [28] shows that within the entire range of pressures from 0 to P_{cr}, the sum $H(T_{boil}) + \Delta Q_w$ differs slightly from the enthalpy of the substance at the critical point. For example, at atmospheric pressure this difference does not exceed 20%. Consequently, we can assume that a decrease in the heat of evaporation to zero is accompanied by a corresponding increase in the enthalpy of the substance at the critical point. In this case, the ratio of the gas parameters determined by the expression $z = RT/(PV)$ increases several-fold. Values of this coefficient are given in [28, 29].

Since monatomic gases, among which are metal vapors, obey the laws of an ideal gas, a similar ratio of them at the temperature of boiling and $P = 10^5$ Pa is of about unity. At present, rather reliable data on critical parameters are available only for substances the boiling temperature of which does not exceed the boiling temperature of water. Even for mercury and alkali metals the error of determination of the critical coefficient cannot reach 50%. By virtue of this, based on the available data we cannot draw an unambiguous conclusion on the presence of a relation between the critical coefficient and the heat content of the substance at the critical point. However, if on the basis of what was said above we assume the existence of a dependence of the form $H(T_{boil}) + \Delta Q_{ev} \approx H(T_{cr}) \approx z_{cr}H(T_{boil})$, we obtain

$$\Delta Q_{ev} \approx (z_{cr} - 1)\, H\,(T_{boil})\,. \tag{52}$$

It follows from Table 5 that the mean value of the critical parameter for alkali metals can be taken ~4.4; therefore, the coefficient 3.4 in (39) for these metals is in agreement with (52).

At present, there are virtually no data on the critical coefficients for materials the melting temperature of which is higher than that of alkali metals. Therefore, in the first approximation, allowing for the results given in Table 3, we can likely take the critical coefficient for materials with a higher temperature of melting and boiling equal to 4.4.

CONCLUSIONS

1. The limiting energy capacity of the inner processes of heat absorption in thermal destruction of a material is established when the thicknesses of the heated and entrained layers are equal and the energy capacity of the entire process of thermal destruction of the material tends to a value equal to the square root of the product of the heat content of the flux and the total thermal effect of surface processes.

2. Numerous experimental data indicate that heating and mass entrainment in thermal destruction of a material are determined by the rate of heating before the onset of melting (destruction) of the surface and do not depend on the aggregate state of the material carried away from the surface. This makes it possible in calculation of the parameters of the nonstationary mode to use the characteristics of stationary destruction (for example, rate of mass entrainment) and shows that in order to increase the economy and efficiency of high-temperature technological processes (for example, separation cutting of materials) it is expedient to increase the thermal power of the jet at the expense of the heat-transfer coefficient (velocity and pressure) of the gas flow rather than its temperature (enthalpy).

3. Since establishment of stationary values of the surface temperature, rate of entrainment, and thickness of the heated layer does not require infinite time of heating, probably it is more precise to use the concept of the "quasistationary mode" relative to the mode of material heating and/or stability of the parameters of external effect.

NOTATION

a, thermal diffusivity, m^2/sec; c, heat capacity, kJ/(kg·K); $\bar{c}_p$ and c_p^{liq}, integral-mean heat capacities of material in the solid and liquid states, kJ/(kg·K); d_0 and $\bar{d}_0$, parameter of nonstationary mass entrainment which specifies displacement of the straight line of linear entrainment relative to the origin of coordinates (m) and its dimensionless value; G_w, evaporation rate, kg/(m^2·sec); $\bar{G}_w$, dimensionless rate of evaporation; G_Σ, rate of mass entrainment, kg/m^2; $\bar{G}_\Sigma$, dimensionless rate of mass entrainment; H, stabilization parameter of mass entrainment, kJ/kg; H^*, parameter of inner heat absorption, kJ/kg; $H(\bar{T})$, heat content of the heated layer, kJ/kg; $H(T_w)$ and $H(T_{boil})$, heat content of the material at the surface temperature and temperature of boiling, kJ/kg; I_e, stagnation enthalpy, kJ/kg; I_w and I_0, gas enthalpy at the temperatures of hot and cold surfaces, kJ/kg; I_{eff}, effective enthalpy of the material, kJ/kg; K, coefficient characterizing the velocity of movement of an isotherm; K_{T_d}, constant of thermal destruction; m, thermal efficiency of the material; m_{er}^*, "threshold" value of the mass of carried-away particles, kg; P and P_{cr}, pressure and its value at the critical point, Pa; P_e, stagnation pressure, Pa; q, heat flux, kW/m^2; q_0, convective heat flux to the hot impermeable surface, kW/m^2; q_w, heat flux with account for injection, kW/m^2; q_{inj}, thermal effect of injection, kW/m^2; q_{cal}, heat flux to the cold surface of the calorimeter, kW/m^2; q_{rad}, radiative heat flux, kW/m^2; $q_0(\tau)$, dependence of heat flux on the time of heating, kW/m^2; R, universal gas constant, J/(kg·K); $S(\tau)$, $S(\tau_v)$, and $S(\tau_\delta)$, linear entrainment and its values at the moment of attainment of quasistationary (stationary) values of the rate of entrainment and thickness of the heated layer, m; $S_k(\tau)$, $S(\tau_k)$, and $S(\tau_{k-1})$, linear entrainment on the kth section of heating and its value at the end of the kth and $(k-1)$th sections of heating, m; $S(T)$ and $S(t_\delta)$, dimensionless linear entrainment and its value at the moment of establishment of the stationary thickness of the heated layer; $S(t_x)$, dimensionless linear entrainment at the moment of its equality to the heated layer; t and t_δ, dimensionless time of heating and its value at the moment of attainment of the stationary thickness of the heated layer; t_x, dimensionless time of heating at the moment of equality of the thicknesses of the heated and entrained layers; T_0, temperature of the nonheated material, K; T_w and $\bar{T}_w$, temperature of the heated surface and its quasistationary (stationary) value, K; T^*, temperature of the isotherm, K; $\bar{T}$, integral-mean temperature of the heated layer, K; $T(y)$, current value of temperature along the coordinate, K; T_d and T_{ent}, temperatures of destruction (melting) and beginning of mass entrainment from the material surface, K; T_{boil} and T_{cr}, temperature of boiling and temperature at the critical point, K; V_∞ and $\bar{V}_\infty$, rate of linear entrainment and its quasistationary (stationary) value, m/sec; $\bar{V}_{\infty i}$, stationary rate of entrainment on the ith section of heating (i = 1, 2, ..., n), m/sec; V_∞ , dimensionless stationary rate of linear entrainment; $V_\theta^*(V_{\theta w})$, velocity of the isotherm (at the surface temperature), m/sec; $\bar{V}_{er}$, velocity of collision of particles with the surface, m/sec; V and V_{cr}, specific volume of a substance and its value at the critical point, m^3/kg; y, coordinate, m; z, dimensionless enthalpy of flow; z_{cr}, critical coefficient; $(\alpha/c_p)_0$ and $(\alpha/c_p)_w$, heat-transfer coefficients without and with account for injection, kg/(m^2·sec); γ, injection parameter; Γ, coefficient of gasification; $\delta_T(\tau)$ and δ_T, depth of the heated layer and its qua-

sistationary (stationary) value, m; $\delta(t)$ and $\bar{\delta}_T$, dimensionless thickness of the heated layer and its value in the stationary mode of heating; $\delta(t_x)$, dimensionless value of the thickness of the heated layer at the moment of its equality to linear entrainment; ΔQ, heat absorbed due to physicochemical conversions on the surface, kJ/kg; ΔQ_w and $(\Delta Q_w)_{max}$, thermal effect of physicochemical conversions on the surface and its maximum value, kJ/kg; $\Delta\varepsilon$, degree of approximation to the asymptote; Δ^* and $\Delta^*(t_\delta)$, total thickness of the entrained and heated layers to the isotherm T^* and its value at the moment of establishment of the quasistationary (stationary) mode of heating, m; $\Delta^*(t)$ and $\Delta^*(t_\delta)$, dimensionless total thickness of the heated and entrained layers and its stationary value; $\Delta\tau_i$, duration of the ith section of heating (i = 1, 2, ..., n), sec; $\Delta\tau_k$, correction to the current time of heating on the kth section, sec; ε, surface emissivity; $\theta^* = (T - T_0)/(T_w - T_0)$, dimensionless temperature of the isotherm; θ_{T_w}, dimensionless value of the surface temperature in its variation from T_d to $\bar{T}_w$; $\theta(y)$, current value of dimensionless temperature; λ, thermal conductivity, W/(m·K); ρ, density, kg/m^3; σ, Stefan–Boltzmann constant, kW/({m^2·K^4); τ, time of heating, sec; τ_1 and τ_2, time of the beginning and termination of the considered period of heating, sec; τ_k and τ_{k-1}, time of termination of the kth and $(k-1)$th sections of heating, sec; τ_T, τ_v, and τ_δ, times of establishment of quasistationary (stationary) values of the surface temperature, rate of mass entrainment, and thickness of the heated layer, sec; τ_ξ, section cut by the linear dependence $\Delta^* = f(\sqrt{\tau})$ on the abscissa axis (τ_ξ = 1 sec); τ_d, time of the onset of destruction (melting) of the surface, sec; τ_{ent}, time of the onset of mass entrainment from the surface, sec; τ_{entk} and τ_{vk}, time of the onset of mass entrainment and time of establishment of the stationary rate of entrainment for the kth section of heating, sec; Ψ, dimensionless heat-transfer function. Indices: 0, nonheated material, impermeable surface; e, outer edge of the boundary layer; k, ordinal number of the nonstationary section of mass entrainment (k = 1, 2, 3, ...); p, pressure; T, temperature; v, velocity; w, conditions on the wall; Σ, total; δ, heated layer; θ^*, dimensionless temperature of the isotherm; inj, injection; liq, liquid; ev, evaporation; cal, calorimetric; boil, boiling; cr, critical value; rad, radiative; d, destruction; melt, melting; mean, integral-mean; ent, mass entrainment; eff, effective; er, erosion; coke, coked; ∞, infinity; max, maximum; min, minimum.

REFERENCES

1. F. I. Zakharov and G. A. Frolov, High-temperature investigation of composite gradient materials in non-equilibrium air plasma, in: *Proc. 3rd Int. Symp. on FGM, Switzerland, Presses Polytechniques et Universitate Romandes*, CH-1015, Lausanne (1995), pp. 413–418.
2. G. Frolov, Application of the high-temperature heating installation for gradient material obtaining, *FGM–News*, Tokyo, Japan, No. 27, 2–5 (1995).
3. G. A. Frolov, V. S. Dvernyakov, V. V. Pasichnyi, and F. I. Zakharov, Heat exchange between subsonic and supersonic plasma jets, *Inzh.-Fiz. Zh.*, **40**, No. 6, 965–969 (1981).
4. V. N. Meshkovskii, V. V. Pasichnyi, G. A. Frolov, A. A. Donskoi, and N. V. Baritko, Helium installations for investigation of heat-accumulating materials, in: *Interband Sci.-Eng. Collection of Papers "Technology"* [in Russian], No. 2, Moscow (1994), pp. 67–70.
5. Yu. V. Polezhaev and G. A. Frolov, Study of the parameters of destruction of heat-protecting materials under conditions of nonstationary heating, *Inzh.-Fiz. Zh.*, **50**, No. 2, 236–240 (1986).
6. Yu. V. Polezhaev and F. B. Yurevich, *Thermal Protection* [in Russian], Énergiya, Moscow (1976).
7. A. V. Luikov, *Heat-Conduction Theory* [in Russian], Vysshaya Shkola, Moscow (1967).
8. G. A. Frolov, Yu. V. Polezhaev, V. V. Pasichnyi, and F. I. Zakharov, Failure parameters of heat-shielding materials in the nonstationary heating regime, *Inzh.-Fiz. Zh.*, **40**, No. 4, 608–614 (1981).
9. W. D. Brewer and P. C. Kassel, Flash x-ray technique for investigation of ablative material response to simulated reentry environments, *Int. J. Nondestructive Testing*, **3**, No. 4, 375–390 (1972).
10. G. A. Frolov, A. A. Korol', V. V. Pasichnyi, V. Ya. Berezhetskaya, E. I. Suzdal'tsev, and V. S. Tsyganenko, Characteristic state-transformation temperatures of quartz glass-ceramic with unidirectional heating, *Inzh.-Fiz. Zh.*, **51**, No. 6, 932–940 (1986).
11. G. A. Frolov and I. A. Podchernyaeva, Improvement of exploitation characteristics of materials by melting of the surface layer in a plasma flow, *Fiz. Khim. Obrab. Mater.*, No. 2, 46–53 (1997).

12. G. A. Frolov, V. V. Pasichnyi, E. I. Suzdal'tsev, and V. S. Tsyganenko, Measurement of temperature fields in specimens of quartz ceramic during surface ablation, *Inzh.-Fiz. Zh.*, **57**, No. 2, 313–317 (1989).
13. G. A. Frolov, V. V. Pasichnyi, Yu. V. Polezhaev, and A. V. Choba, Model of thermal destruction of material subjected to one-sided heating, *Inzh.-Fiz. Zh.*, **52**, No. 1, 33–37 (1987).
14. Yu. V. Polezhaev and G. A. Frolov, Laws governing establishment of a quartz-stationary regime of destruction in one-sided heating of materials, *Inzh.-Fiz. Zh.*, **56**, No. 4, 533–539 (1989).
15. Yu. V. Polezhaev and G. A. Frolov, Influence of thermal conductivity of a material on an unsteady heat removal parameter, *Inzh.-Fiz. Zh.*, **62**, No. 4, 546–551 (1992).
16. M. C. Adams, W. E. Powers, and S. J. Georgiev, An experimental and theoretical study of quartz ablation at the stagnation point, *J. Aero/Space Sci.*, **27**, No. 7, 535–547 (1960).
17. V. L. Sergeev, *Non-Stationary Heat and Mass Transfer in the Region of the Stagnation Point* [in Russian], Nauka i Tekhnika, Minsk (1988).
18. G. A. Frolov, Main laws governing nonstationary mass entrainment in interaction of material with a high-temperature medium, in: *Heat and Mass Transfer–MIF-92* [in Russian], Vol. 3, Minsk (1992), pp. 133–136.
19. G. A. Frolov, Temperature of the surface of a body undergoing destruction by a constant thermal load, *Inzh.-Fiz. Zh.*, **53**, No. 3, 420–426 (1987).
20. Yu. V. Polezhaev and G. A. Frolov, Transient regime in the thermal and erosional destruction of materials, *Inzh.-Fiz. Zh.*, **52**, No. 3, 357–362 (1987).
21. Yu. V. Polezhaev and V. I. Panchenko, Main laws governing the kinetics of erosional destruction of materials, *Inzh.-Fiz. Zh.*, **52**, No. 5, 709–716 (1987).
22. R. I. Harrach, Estimates on the ignition of high-explosive laser pulses, *J. Appl. Phys.*, **47**, No. 6, 2473–2482 (1976).
23. G. A. Frolov, Effect of the type of heating on the rate of destruction of materials, *Inzh.-Fiz. Zh.*, **50**, No. 4, 629–635 (1986).
24. G. A. Frolov, Influence of different factors on evaporation of material in a high-temperature gas flow, in: *Proc. III Minsk Int. Forum "Heat and Mass Transfer–MIF-96"* [in Russian], 20–24 May 1996, Minsk, Vol. 3, Minsk (1996), pp. 55–59.
25. F. B. Yurevich, Behavior of polymer materials in a plasma jet, in: *Heat and Mass Transfer and Thermal Properties of Materials* [in Russian], ITMO AN BSSR, Minsk (1969), pp. 145–154.
26. G. A. Frolov, V. V. Pasichnyi, Yu. V. Polezhaev, A. A. Frolov, and A. V. Choba, Evaluating the fracture energy of a material from its heat content, *Inzh.-Fiz. Zh.*, **50**, No. 5, 709–718 (1986).
27. V. A. Kirillin and A. E. Sheindlin, *Study of Thermodynamic Properties of Substances*, [in Russian], Goséner-gizdat, Moscow–Leningrad (1963).
28. N. B. Vargaftik, *Handbook on Thermophysical Properties of Gases and Liquids* [in Russian], Nauka, Moscow (1972).
29. N. K. Kikoin (Ed.), *Tables of Physical Quantities: Handbook* [in Russian], Atomizdat, Moscow (1976).
30. A. P. Zefirov (Ed.), *Thermodynamic Properties of Inorganic Substances* [in Russian], Atomizdat, Moscow (1965).
31. *Thermodynamic Properties of Individual Substances: Handbook* [in Russian], in 4 vols., Nauka, Moscow (1979–1982).
32. I. V. Kudryavtsev (Ed.), *Materials in Mechanical Engineering* [in Russian], Vol. 1, Mashinostroenie, Moscow (1969).
33. *Encyclopedia of Inorganic Materials* [in Russian], in 2 vols., USÉ, Kiev (1977).
34. V. A. Golovin and E. Kh. Ul'yanova, *Properties of Noble Metals and Alloys* [in Russian], Metallurgiya, Moscow (1964).
35. International Critical Tables of Numerical Data, Physics, Chemistry and Technology, Vol. 1, 2, USA, 1926–1933.
36. G. A. Frolov, Self-organization of heating of materials in heat destruction of its surface, in: *Proc. Int. Conf. "Science for Materials in the Frontier of Centuries: Advantages and Challenges"*, Kiev, 2002, Vol. 2 (2002), pp. 649–650.

37. B. I. Medovar, V. L. Shevtsov, G. S. Marinskii, V. F. Demchenko, and V. I. Makhnenko, *Thermal Processes in Slag Electric Remelting* [in Russian], Naukova Dumka, Kiev (1978).
38. G. A. Frolov, Yu. V. Polezhaev, and V. V. Pasichnyi, Effect of internal and surface processes of heat absorption in the heating and destruction of a material, *Inzh.-Fiz. Zh.*, **53**, No. 4, 533–540 (1987).
39. G. A. Frolov, Yu. V. Polezhaev, and V. V. Pasichnyi, Rate of material destruction in one-sided heating, *Inzh.-Fiz. Zh.*, **52**, No. 4, 533–540 (1987).
40. J. H. Landell and R. R. Dickey, Rate of destruction of materials in one-sided heating, *Raketn. Tekh. Kosmonavt.*, **11**, No. 2, 111–119 (1973).
41. V. V. Kuzmich, Study of destruction of glass-plastics based on silico-fiber and epoxy-binder fillers in quasi-stationary heating, in: *Special Features of Heat and Mass Transfer Processes* [in Russian], ITMO AN BSSR, Minsk (1979), pp. 194–197.
42. Yu. V. Polezhaev, and G. A. Frolov, Laws of thermal disintegration in the interaction of a body with a high-speed gas flow, *Inzh.-Fiz. Zh.*, **57**, No. 3, 357–363 (1989).
43. V. V. Gorskii and S. T. Surzhikov, Fracture characteristics of glass-graphite bodies in a partially ionized air flow, *Inzh.-Fiz. Zh.*, **42**, No. 4, 640–645 (1982).
44. Yu. V. Polezhaev (K. V. Frolov Ed.), in: *Mechanical Engineering: Encyclopedia* [in Russian], Vols. 1–2, Mashinostroenie, Moscow (2001), pp. 463–467.
45. G. A. Frolov, Limit power consumption of major factors of heat absorption at thermal destruction of the material, in: *Proc. 2nd Int. Conf. "Materials and Coatings for Extreme Performances: Investigation, Applications, Ecologically Safe Technologies for Their Production and Utilization*," Ukraine, Crimea, Kiev (2002), pp. 17–18.
46. V. E. Abaltusov, Study of the characteristics of destruction of glass-graphite bodies in a partially ionized air flow, *Izv. Sib. Otd. Akad. Nauk SSSR, Ser. Tekh. Nauk*, No. 10, Issue 2, 10–13 (1985).
47. V. S. Avduevskii and G. A. Glebov, Heat exchange in the neighborhood of the stagnation point on a permeable surface, *Inzh.-Fiz. Zh.*, **18**, No. 5, 777–782 (1970).
48. N. A. Anfimov and V. V. Al'tov, Heat transfer, friction, and mass transfer in a laminar multicomponent boundary layer with injection of foreign gases, *Teplofiz. Vys. Temp.*, **3**, No. 3, 409–420 (1965).
49. V. P. Mugalev, Effect of injection of different gases on heat transfer near the front critical point of a blunt body, *Izv. Akad. Nauk SSSR, Mekh. Zhidk. Gaza*, No. 1, 175–180 (1965).
50. R. N. Feldhuhm, Heat transfer from a turbulent boundary layer on porous hemisphere, *AIAA Paper*, No. 119 (1976).
51. Yu. V. Polezhaev, *Methods and Means of Gasdynamic Tests of Flying Vehicles* [in Russian], MAI, Moscow (1983).
52. A. P. Vinogradov, *Geokhimiya*, No. 11, 1283–1286 (1971).
53. G. V. Voitkevich, *Origin and Chemical Evolution of the Earth* [in Russian], Nauka, Moscow (1973).